SIAM J. Applied Dynamical Systems
Vol. 17, No. 1, pp. 823–858

Sliding and Crossing Dynamics in Extended Filippov Systems*

Mate Antali† and Gabor Stepan†

Abstract. In spatial contact problems of rigid bodies, Coulomb friction results in dynamical systems with codimension-2 discontinuity manifolds, which are outside the scope of piecewise smooth dynamical systems. This motivated the authors to extend Filippov systems to codimension-2 discontinuity manifolds, which leads to the definition of extended Filippov systems. In these systems, sliding and crossing regions can be defined analogously to those of standard Filippov systems. A convex construction of the sliding vector is also presented in the paper. The developed methods are demonstrated on mechanical problems with spatial Coulomb friction.

Key words. Filippov system, sliding, nonsmooth, discontinuous, codimension

AMS subject classifications. 34A36, 34C99, 37N05, 70F40

DOI. 10.1137/17M1110328

1. Introduction.

In the field of the theory of piecewise smooth systems, many concepts and tools have been developed in the last decades. One of the main classes of piecewise smooth systems is Filippov systems where the vector field has discontinuity on some switching surfaces of the phase space. The first substantial theory was developed by Filippov [11]. A thorough overview of Filippov systems and further references can be found in the handbook of di Bernardo and co-authors [6].

Filippov systems can be used for many applications in mechanics and control. Coulomb friction is one of the fundamental effects which provide a discontinuity leading to Filippov systems. This occurs at *planar* contact problems of rigid bodies when the discontinuity occurs on a codimension-1 switching surface determined by the zero relative velocity at the contact point. However, in *spatial* contact problems of rigid bodies, Coulomb friction results in discontinuity when both components of the relative velocity are zero *at the same time* (see, e.g., [22]). This results in a codimension-2 discontinuity surface, and thus, the resulting dynamical system is outside the scope of Filippov systems and even of piecewise smooth systems.

This spatial Coulomb friction gives the motivation to *extend* the concepts and tools of Filippov systems to the case when there is a codimension-2 discontinuity set in the phase space. In this paper, the usual Filippov systems with codimension-1 discontinuities are called *simple* Filippov systems, and we introduce the term *extended* Filippov systems to the case of codimension-2 discontinuity manifolds.

*Received by the editors January 3, 2017; accepted for publication (in revised form) by J. Sieber November 21, 2017; published electronically March 27, 2018.
http://www.siam.org/journals/siads/17-1/M111032.html
Funding: This research was supported by the European Research Council under the European Union's Seventh Framework Programme (FP/2007-2013)/ERC Advanced Grant Agreement 340889.
†Budapest University of Technology and Economics, Budapest, Hungary (antali@mm.bme.hu, stepan@mm.bme.hu).

Note, that the framework of complementary problems and set-valued force laws can also be used to analyze discontinuous mechanical systems with spatial Coulomb friction (see [12], [13], [19], and [5]). However, this paper uses a different approach: we extend the framework of piecewise smooth systems to include the systems with codimension-2 discontinuities.

It is important to distinguish the present extension from the analysis of Dieci and coauthors [9, 8, 7] and Jeffrey [15]. In those papers, the dynamics at the intersection of two switching surfaces is analyzed in simple Filippov systems. This situation also provides codimension-2 discontinuity manifolds, as an intersection of two codimension-1 discontinuity sets. In contrast, in this paper, we consider *isolated* codimension-2 discontinuities.

The structure of the paper is the following: In section 2, a short overview of simple Filippov systems is presented, and some new concepts are defined which are used subsequently. In section 3, the concept of extended Filippov systems is introduced which contain codimension-2 manifolds in the phase space. In section 4, the different possibilities of the behavior of the trajectories is explored at the discontinuity set. In section 5, we define sliding and crossing regions of the codimension-2 discontinuity sets and we present the construction of the sliding dynamics. In section 6, the application of the theory is demonstrated on mechanical examples with spatial Coulomb friction.

2. Simple Filippov systems—The codimension-1 case.

In this section, we take a short overview of Filippov systems to have the necessary basis to the following analysis. In subsection 2.1, the most important concepts of Filippov systems are summarized from the literature. We mainly follow the notation of [6]. In subsection 2.2, we introduce a few new concepts which are used later for the extension to codimension-2 discontinuity sets.

2.1. Overview of Filippov systems.

2.1.1. Codimension-1 discontinuity manifolds. Let us consider an open set $\mathcal{D} \subset \mathbb{R}^m$ and an $m-1$ dimensional smooth manifold $\Sigma \subset \mathcal{D}$. The manifold can be generated as a zero set of a smooth function $H : \mathcal{D} \to \mathbb{R}$, that is,

$$\Sigma = \{x \in \mathcal{D} : H(x) = 0\}. \tag{2.1}$$

We require that the gradient ∇H of H does not vanish anywhere in Σ. Then, for each $x_0 \in \Sigma$, the two unit vectors orthogonal to Σ are

$$n_1(x_0) := \frac{\nabla H(x_0)}{\|\nabla H(x_0)\|}, \qquad n_2(x_0) := -n_1(x_0), \tag{2.2}$$

where $\|.\|$ is the usual 2-norm on $\mathbb{R}^m$.

The manifold divides $\mathcal{D}$ into two regions,

$$\begin{aligned} S_1 &:= \{x \in \mathcal{D} : H(x) > 0\}, \\ S_2 &:= \{x \in \mathcal{D} : H(x) < 0\}, \end{aligned} \tag{2.3}$$

where $S_1 \cup S_2 \cup \Sigma = \mathcal{D}$. (See the left panel of Figure 1.) The term *piecewise smooth system* is used for vector fields on $\mathbb{R}^m$ when the flow of the system is smooth in S_1 and S_2, but it is nonsmooth on Σ. Then, Σ is called the *discontinuity manifold* or *switching manifold* of the system. According to the type of the discontinuity, we can speak about hybrid systems, Filippov systems, and continuous piecewise smooth systems (see [6, p. 73]).

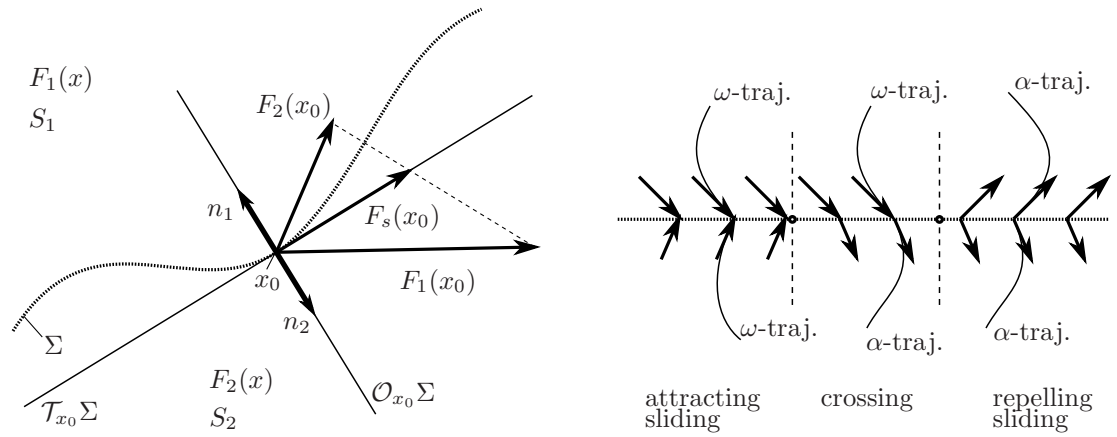

Figure 1. *Concept of codimension-1 discontinuity manifold (switching manifold). Left panel: basic concepts of Filippov system. Right panel: typical types of behavior at the discontinuity manifold. In each region, a pair of typical limit trajectories are depicted. The tangency points are denoted by dots.*

2.1.2. Basic notation of Filippov systems.

Let us consider the differential equation

$$\dot{x} = F(x), \tag{2.4}$$

where the vector field $F : \mathcal{D} \setminus \Sigma \to \mathbb{R}^m$ can be written into the form

$$F(x) = \begin{cases} F_1(x), & x \in S_1, \\ F_2(x), & x \in S_2, \end{cases} \tag{2.5}$$

and F_1, F_2 are smooth vector fields on $S_1 \cup \Sigma$ and $S_2 \cup \Sigma$, respectively. Moreover, we require $F_1(x_0) \neq F_2(x_0)$ for all $x_0 \in \Sigma$. That is, the discontinuity at Σ is uniform with degree one (see [6, p. 73]), and thus, (2.5) is a Filippov system.

The discontinuity manifold Σ has two typical regions according to the direction of the surrounding trajectories. (See the right panel of Figure 1.)

Definition 2.1 (sliding region). *The sliding region of Σ is the set of points $x_0 \in \Sigma$ for either $\langle F_i, n_i \rangle (x_0) < 0$ for all $i \in \{1, 2\}$ or $\langle F_i, n_i \rangle (x_0) > 0$ for all $i \in \{1, 2\}$. The sliding region is denoted by $\Sigma_{sl} \subset \Sigma$.*

Definition 2.2 (crossing region). *The crossing region of Σ is the set of points $x_0 \in \Sigma$ for the fact that there exists $i, j \in \{1, 2\}$ with $\langle F_i, n_i \rangle (x_0) > 0$ and $\langle F_j, n_j \rangle (x_0) < 0$. The crossing region is denoted by $\Sigma_{cr} \subset \Sigma$.*

The bracket $\langle ., . \rangle$ denotes the usual scalar product on $\mathbb{R}^m$. The sliding region is called *attracting* if $\langle F_i, n_i \rangle (x_0) < 0$ for all $i \in \{1, 2\}$ and it is called *repelling* if $\langle F_i, n_i \rangle (x_0) > 0$ for all $i \in \{1, 2\}$. Points of boundaries between sliding and crossing regions form a further subset of Σ, where either F_1 or F_2 is tangent to the discontinuity set.

Definition 2.3 (tangency point). *A point $x_0 \in \Sigma$ is called a tangency point if there exists $i \in \{1, 2\}$ with $\langle F_i, n_i \rangle (x_0) = 0$. The set of tangency points is denoted by $\Sigma_{ta} \subset \Sigma$.*

These three types of points cover the whole discontinuity set, that is, $\Sigma_{sl} \cup \Sigma_{cr} \cup \Sigma_{ta} = \Sigma$.

2.1.3. Sliding dynamics. In the crossing region, trajectories of F_1 and F_2 can be concatenated to obtain a trajectory of F. However, in the sliding region, the trajectories cannot be continued through Σ and they get stuck in Σ in forward or backward time. Then, the vector field F can be extended to the discontinuity set by introducing the *sliding vector field* $F_s : \Sigma_{sl} \to \mathbb{R}^m$, which is required to be tangent to Σ.

The most straightforward method to construct the sliding dynamics is Filippov's convex method (introduced in [11]), which considers simply the convex combination of F_1 and F_2 in the form

$$F_s := (1-\alpha)\, F_1 + \alpha F_2 \tag{2.6}$$

with $\alpha \in \mathbb{R}$. The convex combination can be also expressed in the form

$$F_s = \frac{F_1 + F_2}{2} + \beta \frac{F_2 - F_1}{2}, \tag{2.7}$$

where $\beta = 2\alpha - 1$. In the literature, (2.6) is sometimes called Filippov's form of the sliding vector while (2.7) is called Utkin's form (see [6, p. 77]). The convex combination requires $0 \le \alpha \le 1$, which corresponds to $-1 \le \beta \le 1$.

If there is additional explicit information about the dynamics in the sliding region, then the sliding dynamics can be expressed in a more general form than (2.6) by using nonconvex combination. This can be done, e.g., by Utkin's equivalent control method [23]. In this paper, we restrict ourselves to the concept of *convex* combination in the forms (2.6) or (2.7). (See the left panel of Figure 1.)

The parameters $\alpha(x_0)$ and $\beta(x_0)$ have to be chosen to have a resulting sliding vector F_s being tangent to Σ at any $x_0 \in \Sigma_{sl}$. This can be expressed by $\langle F_s, n_1 \rangle (x_0) = 0$, which leads to

$$\alpha(x_0) = \frac{\langle F_1, n_1 \rangle}{\langle F_1, n_1 \rangle + \langle F_2, n_2 \rangle}(x_0) \tag{2.8}$$

and

$$\beta(x_0) = \frac{\langle F_1, n_1 \rangle - \langle F_1, n_2 \rangle}{\langle F_1, n_1 \rangle + \langle F_1, n_2 \rangle}(x_0). \tag{2.9}$$

In the sliding region Σ_{sl}, we have $0 < \alpha < 1$ (or $-1 < \beta < 1$), which we can call *nontrivial convex combination* because $F_s \neq F_i$ for all $i \in \{1, 2\}$.

2.2. Establishing extension to the codimension-2 case. In this subsection, we introduce some new concepts and notation for Filippov systems which will be used in the subsequent sections to extend the concept of Filippov systems to codimension-2 discontinuity sets.

2.2.1. Set of orthogonal directions. At a point $x_0 \in \Sigma$ of the discontinuity set, let $\mathcal{T}_{x_0}\Sigma$ denote the tangent space of Σ, and let $\mathcal{O}_{x_0}\Sigma$ denote its orthogonal complement defined by

$$\mathcal{O}_{x_0}\Sigma := \{v \in \mathbb{R}^m : \langle v, w \rangle = 0;\ \forall w \in \mathcal{T}_{x_0}\Sigma\}\,. \tag{2.10}$$

That is, $\mathcal{O}_{x_0}\Sigma$ contains the vectors that are normal to Σ at x_0. (See the left panel of Figure 1.)

Let $E(x_0)$ denote the set of *unit vectors* in the orthogonal space at x_0, that is,

$$E(x_0) := \{n \in \mathcal{O}_{x_0}\Sigma : \|n\| = 1\}. \tag{2.11}$$

As $\mathcal{O}_{x_0}\Sigma$ is one dimensional (1D), $E(x_0)$ contains two elements: $E(x_0) = \{n_1(x_0), n_2(x_0)\}$, vectors are defined in (2.2). Each unit vector can be identified with its direction, and thus, we can refer to $n_i(x_0)$ simply as a *direction* orthogonal to Σ and $E(x_0)$ can be called the set of orthogonal directions. Elements $n_i(x_0)$ of $E(x_0)$ are referred to by the indices $i \in \{1, 2\}$.

2.2.2. Directional limits of the vector field. The vector field F is not defined in Σ but the limits

$$F_i^*(x_0) := \lim_{\epsilon \to 0^+} F\big(x_0 + \epsilon n_i(x_0)\big) = F_i(x_0) \tag{2.12}$$

exist for $i \in \{1, 2\}$. We call F_1^* and F_2^* the *directional limits* with respect to the directions n_1 and n_2, respectively. These directional limits will play an important role in subsection 3.2 when considering codimension-2 discontinuity manifolds.

2.2.3. Limit trajectories. Let us define the following two types of trajectories that approach points of the discontinuity set in forward or backward time.

Definition 2.4 (ω-trajectory). *Consider a point $x_0 \in \Sigma$ and a trajectory $\gamma : (t_0, t_1) \to \mathbb{R}^m$ of F. Suppose that $\lim_{t \to t_1} \gamma(t) = x_0$, and $\lim_{t \to t_1} \langle F(\gamma(t)), n_1(x_0)\rangle \neq 0$. Then, γ is called an ω-trajectory of x_0 with respect to the dynamics of F.*

This means that ω-trajectories tend to x_0 in *finite* time in the forward direction of time. The condition with the scalar product is required to exclude trajectories that are tangent to $\mathcal{T}_{x_0}\Sigma$ at x_0. Similarly, we can define trajectories tending to x_0 in finite time in the backward direction of time.

Definition 2.5 (α-trajectory). *Consider a point $x_0 \in \Sigma$ and a trajectory $\gamma : (t_0, t_1) \to \mathbb{R}^n$ of F. Suppose that $\lim_{t \to t_0} \gamma(t) = x_0$, and $\lim_{t \to t_0} \langle F(\gamma(t)), n_1(x_0)\rangle \neq 0$. Then, γ is called an α-trajectory of x_0 with respect to the dynamics of F.*

The α- and ω-trajectories of x_0 are called the *limit trajectories* of x_0. The number and type of limit trajectories characterize the subsets Σ_{sl}, Σ_{cr}, and Σ_{ta} of the discontinuity set. In the sliding and crossing regions, any point x_0 has 2 limit trajectories. In case of tangency points, there are 0 or 1 limit trajectories.

In the crossing region, a point x_0 has an α-trajectory and an ω-trajectory, which can be connected together to obtain a trajectory of F crossing the discontinuity surface. In the sliding region, a point x_0 has either two α-trajectories (repelling sliding) or two ω-trajectories (attracting sliding), and thus, the trajectories reach the discontinuity manifold in forward or backward time. These trajectories can be continued with the sliding dynamics. Some typical limit trajectories are depicted in the right panel of Figure 1.

2.2.4. Equivalent definitions of sliding region. In the literature, sliding region is usually defined by Definition 2.1 (see, e.g., [6, p. 76]). However, other definitions could also be used as is stated by the following proposition.

Proposition 2.6 (equivalence of three definitions of the sliding region). *For a point $x_0 \in \Sigma$, the following three statements are equivalent:*

(a) *either $\langle F_i, n_i \rangle (x_0) < 0$ for all $i \in \{1,2\}$ or $\langle F_i, n_i \rangle (x_0) > 0$ for all $i \in \{1,2\}$;*
(b) *there exists a sliding vector $F_s(x_0)$ with $0 < \alpha(x_0) < 1$;*
(c) *x_0 has either two α-trajectories or two ω-trajectories with respect to F.*

The proof if straightforward: Equivalence of (a) and (b) can be proved from (2.8), and equivalence of (a) and (c) can be proved by considering the trajectories of F_1 and F_2 at x_0. However, we will see in subsection 5.4 that although statements of Proposition 2.6 can be all extended to the codimension-2 case, the generalized statements are *not* equivalent.

2.2.5. Compact form of constructing the sliding dynamics. Let us rewrite the formulae (2.6) and (2.7) to have expressions easy to extend to the codimension-2 case. By introducing $\alpha_1 := 1 - \alpha$ and $\alpha_2 := \alpha$, the formula (2.6) can be written in the form

$$F_s = \sum_{i=1}^{2} \alpha_i F_i, \qquad \sum_{i=1}^{2} \alpha_i = 1. \tag{2.13}$$

In this form, the sliding vector field is expressed as the weighted average of F_1 and F_2, where the weights α_1 and α_2 depend on the location x_0 in the sliding region. Similarly, let $\beta_1 := -\beta$, $\beta_2 := \beta$. Then, (2.7) can be written into the form

$$F_s = \overline{F} + \tfrac{1}{2} \sum_{i=1}^{2} \beta_i \left(F_i - \overline{F} \right), \qquad \sum_{i=1}^{2} \beta_i = 0, \tag{2.14}$$

where

$$\overline{F} := \tfrac{1}{2} \sum_{i=1}^{2} F_i. \tag{2.15}$$

In this form, the sliding vector field is expressed as the average $\overline{F}$ of the vector fields F_1 and F_2 plus the weighted average of the deviations from the average with the weights β_1 and β_2, where $\beta_i = 2\alpha_i - 1$.

3. Extended Filippov systems—Extension to the codimension-2 case. The manifold Σ of simple Filippov systems can be called either a *switching manifold* between F_1 and F_2 or a *discontinuity manifold* of F (see (2.5)). These two names for the same notion refer to slightly different approaches to the system. The term *switching manifold* emphasizes that regions of smooth dynamics are *separated* by this manifold. The term *discontinuity manifold* emphasizes that the manifold is embedded *into* the region of smooth dynamics.

These two points of view lead to different ways to extend to higher codimension cases. Taking the intersection of two switching manifolds leads to systems analyzed by Dieci and Lopez [9] and Jeffrey [15]. Then, a codimension-2 discontinuity manifold is generated by the intersection of the codimension-1 switching surfaces. However, we can also consider a discontinuity on a single codimension-2 discontinuity manifold, which leads to the systems analyzed in the present paper.

3.1. Codimension-2 isolated discontinuity manifolds. Let us consider the open set $\mathcal{D} \subset \mathbb{R}^m$ and the $m-2$ dimensional smooth manifold $\Sigma \subset \mathcal{D}$. The manifold can be defined in the form

$$\Sigma = \{x \in \mathcal{D} : H_j(x) = 0, j = 1, 2\}, \tag{3.1}$$

where each $H_j : \mathcal{D} \to \mathbb{R}$ is a smooth function having gradients $\nabla H_j(x_0) \neq 0$ that satisfy $\langle \nabla H_1, \nabla H_2 \rangle (x_0) = 0$ for all $x_0 \in \Sigma$. At a point $x_0 \in \Sigma$, let $\mathcal{T}_{x_0}\Sigma$ be the tangent space of Σ and let $\mathcal{O}_{x_0}\Sigma$ be its orthogonal complement defined as in (2.10). In this case, $\mathcal{T}_{x_0}\Sigma$ is $m-2$ dimensional and $\mathcal{O}_{x_0}\Sigma$ is 2D.

As in (2.11), let

$$E(x_0) := \{n \in \mathcal{O}_{x_0}\Sigma : \|n\| = 1\} \tag{3.2}$$

be the set of unit vectors in $\mathcal{O}_{x_0}\Sigma$. In the codimension-1 case of simple Filippov systems, the 1D orthogonal space contained only two unit vectors. In contrast, in the codimension-2 case, there are continuously many unit vectors in $\mathcal{O}_{x_0}\Sigma$; the elements of $E(x_0)$ form a unit circle.

To express the elements of $E(x_0)$ explicitly, let us define

$$n_{(1)}(x_0) := \frac{\nabla H_1(x_0)}{\|\nabla H_1(x_0)\|}, \qquad n_{(2)}(x_0) := \frac{\nabla H_2(x_0)}{\|\nabla H_2(x_0)\|}, \tag{3.3}$$

which provide an orthonormal basis of $\mathcal{O}_{x_0}\Sigma$. Then, the periodic function

$$n(\phi)(x_0) := \cos(\phi)\, n_{(1)}(x_0) + \sin(\phi)\, n_{(2)}(x_0) \tag{3.4}$$

can be defined which maps the interval $[0, 2\pi)$ onto the set $E(x_0)$ of unit normal vectors. (See the right panel of Figure 2.) The parameter ϕ expresses the angle between $n_{(1)}$ and $n(\phi)$. Thus, we can refer to ϕ as a *direction* in the orthogonal space. The basis vectors $n_{(1)}$ and $n_{(2)}$ generate a local coordinate system in the orthogonal space $\mathcal{O}_{x_0}\Sigma$ by

$$x_{(1)} := \langle x - x_0, n_{(1)} \rangle, \qquad x_{(2)} := \langle x - x_0, n_{(2)} \rangle. \tag{3.5}$$

In this paper, we investigate vector fields which are smooth in the vicinity of the manifold Σ but that have discontinuity on Σ.

3.2. Definition of extended Filippov systems. Let us now extend Filippov systems to codimension-2 discontinuities. Consider the dynamical system

$$\dot{x} = F(x), \tag{3.6}$$

where F is a vector field $F : \mathcal{D} \setminus \Sigma \to \mathbb{R}^m$ and Σ is an $m-2$ dimensional manifold in $\mathcal{D}$. Analogously to (2.12), let us define the limit

$$F^*(\phi)(x_0) := \lim_{\epsilon \to 0^+} F\left(x_0 + \epsilon n(\phi)(x_0)\right). \tag{3.7}$$

Then, we can introduce the following definition that is the center concept of the analysis in this paper.

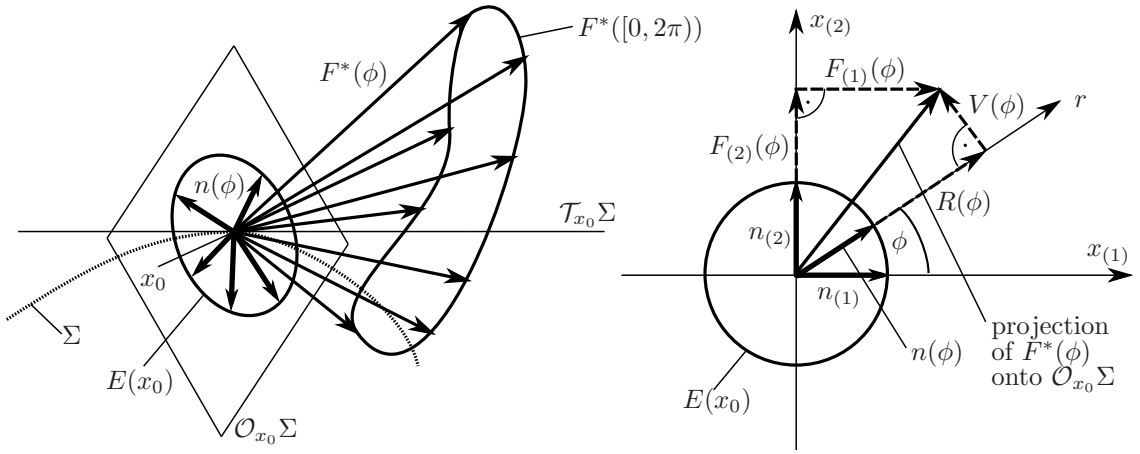

Figure 2. *Vector field at a codimension-2 discontinuity manifold of extended Filippov systems. Left panel: the vector field in the vicinity of a point $x_0 \in \Sigma$. For each angle $\phi \in [0, 2\pi)$, the unit normal vector $n(\phi)$ is used to calculate the limit $F^*(\phi)$ of the vector field. Right panel: coordinate systems and components of the limit vector $F^*(\phi)$ in the orthogonal space.*

Definition 3.1 (extended Filippov system). *Consider the $m-2$ dimensional smooth manifold Σ in $\mathcal{D} \subset \mathbb{R}^m$ and the vector field $F : \mathcal{D} \setminus \Sigma \to \mathbb{R}^m$. Assume that F is smooth on $\mathcal{D} \setminus \Sigma$. Moreover, assume that for all $x_0 \in \Sigma$,*

(a) *the limit $F^*(\phi)(x_0)$ exists for all $\phi \in [0, 2\pi)$, and*

(b) *there exists $\phi_1, \phi_2 \in [0, 2\pi)$ with $F^*(\phi_1)(x_0) \neq F^*(\phi_2)(x_0)$.*

Then, we call F an extended Filippov system *and we call Σ a* codimension-2 isolated discontinuity manifold *of F.*

This construction results in a natural generalization of simple Filippov systems to the codimension-2 case. (See the left panel of Figure 2.) The properties (a)–(b) in Definition (b) are analogous to the condition of uniform discontinuity with degree one which is required in simple Filippov systems.

A vector field with this kind of discontinuity is *not* a piecewise smooth system. In this case, there is no switching between different types of dynamics, but the vector field is smooth everywhere around the discontinuity surface. In the meantime, we get *continuously many* types of behavior of the system if we approach the discontinuity set from different directions of $n(\phi)$ (see Figure 2). At a given point $x_0 \in \Sigma$, the vector field $F^*(\phi)$ maps the set $[0, 2\pi)$ into $\mathbb{R}^m$, which we call the *limit vector field* of F at x_0. The properties of F and n induce that $F^*(\phi)(x_0)$ depends smoothly on both variables.

If property (b) in Definition 3.1 were released and if we allowed a constant limit vector field $F^*(\phi)$, then we would include vector fields which are continuous on Σ but there is still discontinuity in the derivatives. This case would be the codimension-2 generalization of piecewise smooth continuous vector fields, but these systems are not considered in this paper.

The term *isolated* discontinuity set is used to distinguish this type of singularity from the intersection of codimension-1 manifolds in Filippov systems (see [9] and [15]). In those systems, the resulting codimension-2 discontinuity manifold is not isolated but it is embedded into the

codimension-1 discontinuity manifolds. In this paper, we consider isolated discontinuities described in Definition 3.1. We omit the term *isolated* where it is not necessary to emphasis this difference.

The term extended Filippov system could be replaced by the term codimension-2 Filippov system. However, that term would be ambiguous because systems in Definition 3.1 are *not* Filippov systems in the classical sense but they provide a new set of nonsmooth dynamical systems. It must be possible to analyze simple Filippov systems, extended Filippov systems, and higher codimension cases in a common framework, but this project is outside the scope of this paper.

4. Limit trajectories of extended Filippov systems. In the codimension-2 case, we can introduce similar definitions of α-trajectories and ω-trajectories as we did in Definitions 2.4–2.5 for simple Filippov systems.

Definition 4.1 (ω-trajectory in an extended Filippov system). *Consider a point $x_0 \in \Sigma$ and a trajectory $\gamma : (t_0, t_1) \to \mathbb{R}^m$ of F. Suppose that $\lim_{t\to t_1} \gamma(t) = x_0$, and there does not exist any $v \in \mathcal{T}_{x_0}\Sigma$ for that $\lim_{t\to t_1} F(\gamma(t)) = v$. Then, γ is called an ω-trajectory of x_0 with respect to the dynamics of F.*

Definition 4.2 (α-trajectory in an extended Filippov system). *Consider a point $x_0 \in \Sigma$ and a trajectory $\gamma : (t_0, t_1) \to \mathbb{R}^n$ of F. Suppose that $\lim_{t\to t_0} \gamma(t) = x_0$, and there does not exist any $v \in \mathcal{T}_{x_0}\Sigma$ for that $\lim_{t\to t_0} F(\gamma(t)) = v$. Then, γ is called an α-trajectory of x_0 with respect to the dynamics of F.*

In the definitions, we exclude the special cases when a trajectory approaches x_0 from any direction in the tangent space. The set of *limit trajectories* of $x_0 \in \Sigma$ consist of the corresponding α-trajectories and ω-trajectories. To determine the occurrence of these trajectories, we transform the vector field F first into polar coordinates. Then, the time scale is transformed to resolve the discontinuity. This is a similar process to the method of polar blowup (see [10] or [18, p. 160]).

Let us define the functions

$$F_{(1)}(\phi) := \left\langle F^*(\phi), n_{(1)} \right\rangle, \qquad F_{(2)}(\phi) := \left\langle F^*(\phi), n_{(2)} \right\rangle, \tag{4.1}$$

where $F_{(1)}$ and $F_{(2)}$ are the components of the limit vector field $F^*(\phi)$ with respect to the basis vectors of the orthogonal space $\mathcal{O}_{x_0}\Sigma$. (See the right panel of Figure 2.) The projected vector field (4.1) can be expressed in a coordinate system fixed to $n(\phi)$, and we get

$$\begin{aligned} R(\phi) &:= \langle F^*(\phi), n(\phi) \rangle = F_{(1)}(\phi)\cos\phi + F_{(2)}(\phi)\sin\phi, \\ V(\phi) &:= \langle F^*(\phi), n(\phi + \pi/2) \rangle = F_{(2)}(\phi)\cos\phi - F_{(1)}(\phi)\sin\phi. \end{aligned} \tag{4.2}$$

From (4.2), the planar dynamical system

$$\begin{pmatrix} \dot{r} \\ \dot{\phi} \end{pmatrix} = \begin{pmatrix} R(\phi) \\ V(\phi)/r \end{pmatrix} \tag{4.3}$$

can be constructed where the variables $(r, \phi) \in \mathbb{R}^+ \times [0, 2\pi)$ are polar coordinates in the orthogonal space. Formally, we let $\phi \in \mathbb{R}$ in the calculations, but we identify ϕ with $\phi + 2h\pi$ for

any integer h to remain in the interval $[0, 2\pi)$. In the vicinity of x_0, (4.3) describes the dynamics of $F(x)$ projected into the orthogonal space $\mathcal{O}_{x_0}\Sigma$. Corresponding to the discontinuity of F at x_0, the system (4.3) has a discontinuity at the line $r = 0$ in the phase plane (r, ϕ) of (4.3). We are interested in the trajectories of (4.3) when $r \to 0$.

To get an auxiliary system without the singularity at $r = 0$, let us transform the time t to a new time variable τ; this transformation can be defined by the initial condition problem

$$\frac{\mathrm{d}t(\tau)}{\mathrm{d}\tau} = r(\tau), \qquad t(\tau)_{\tau=0} = 0. \tag{4.4}$$

Then, (4.3) becomes

$$\begin{pmatrix} \mathrm{d}r/\mathrm{d}\tau \\ \mathrm{d}\phi/\mathrm{d}\tau \end{pmatrix} = \begin{pmatrix} rR(\phi) \\ V(\phi) \end{pmatrix}, \tag{4.5}$$

which is defined also for $r = 0$. If we exclude the special case when $R(\phi)$ and $V(\phi)$ have common zeroes; then the fixed points of (4.5) are given by $r = 0$ and $V(\phi) = 0$.

4.1. Case of existing limit directions. Consider the case when $V(\phi_i) = 0$ for $i = 1 \dots k$. Then, the k fixed points of (4.3) are $(0, \phi_i)$, and the Jacobian of (4.3) at ϕ_i is

$$J_i = \begin{pmatrix} R(\phi_i) & 0 \\ 0 & V'(\phi_i) \end{pmatrix}, \tag{4.6}$$

where the dash $'$ denotes differentiation with respect to ϕ. The eigenvalues are $R(\phi_i)$ and $V'(\phi_i)$, and the eigenvectors are the directions of the r and ϕ coordinates, respectively. The eigenspace of $R(\phi)$ is the half line determined by $\phi = \phi_i$ and $r \geq 0$, and we can state the following proposition to describe the solutions of (4.3) on this half line.

Proposition 4.3. *Let $(0, \phi_i)$ be a fixed point of (4.5) with $R(\phi_i) \neq 0$ and let $r_0 \in \mathbb{R}^+$. Then, the trajectory of (4.3) passing through (r_0, ϕ_i) tend to $(0, \phi_i)$ in finite time in the forward or backward direction of time.*

Proof. In the case $R(\phi_i) < 0$, the initial condition leads to the solution

$$\begin{pmatrix} r(\tau) \\ \phi(\tau) \end{pmatrix} = \begin{pmatrix} r_0 \exp(R(\phi_i)\tau) \\ \phi_i \end{pmatrix} \tag{4.7}$$

of (4.5), which converges to $(0, \phi_i)$ when $\tau \to \infty$. By (4.4), the time variable τ can be transformed back to the original time variable t of (4.3). Then, the time of approaching $r = 0$ becomes

$$\lim_{\tau\to\infty} t(\tau) = \lim_{\tau\to\infty} \int_0^\tau \frac{\mathrm{d}t(s)}{\mathrm{d}s}\mathrm{d}s = \lim_{\tau\to\infty} \int_0^\tau r(\tau)\mathrm{d}s = \frac{-r_0}{R(\phi_i)}, \tag{4.8}$$

which is a positive real number. The case $R(\phi_i) > 0$ can be proved analogously by calculating the limit at $\tau \to -\infty$. ∎

The consequence of Proposition 4.3 is that for each ϕ_i with $V(\phi_i) = 0$ and $R(\phi_i) \neq 0$, the point x_0 possesses a limit trajectory with respect to F. Hence, we can call such a ϕ_i direction a *limit direction* of x_0. If $R(\phi_i) < 0$, then the solution (4.7) corresponds to an ω-trajectory of x_0, and if $R(\phi_i) > 0$, then (4.7) is related to an α-trajectory of x_0. In these cases, the limit direction ϕ_i is called an *attracting direction* or a *repelling direction* of x_0, respectively. In the special case $R(\phi_i) = 0$, (4.7) becomes an *constant* solution and hence, ϕ_i is not a limit direction of x_0.

If $R(\phi_i) \cdot V'(\phi_i) < 0$, then $(0, \phi_i)$ is a saddle, and if $R(\phi_i) \cdot V'(\phi_i) \geq 0$, then $(0, \phi_i)$ is a node or a degenerate saddle-node. In case of the saddle, (4.7) is the only trajectory of (4.5) which tends to $(0, \phi_i)$ in forward or backward direction of time, that is, the attracting or repelling direction ϕ_i corresponds to a single ω- or α-trajectory of x_0, respectively. In case of the node and the saddle-node, infinitely many trajectories tend to $(0, \phi_i)$, that is, the attracting or repelling direction ϕ_i corresponds to continuously many ω- or α-trajectories of x_0, respectively.

We demonstrate these results on two examples.

Example 4.4 (system with attracting directions). Consider the system

$$F(x_1, x_2, x_3) = \begin{pmatrix} -\frac{x_1}{\sqrt{x_1^2+x_2^2}} + \frac{3}{2} \cdot \frac{x_1 x_2}{x^2+x_2^2} + \frac{1}{2} \\ -\frac{x_2}{\sqrt{x_1^2+x_2^2}} + \frac{3}{2} \cdot \frac{x_2^2}{x^2+x_2^2} \\ -x_3 \end{pmatrix} \tag{4.9}$$

with $(x_1, x_2, x_3) \in \mathcal{D} = \mathbb{R}^3 \setminus \Sigma$, where the discontinuity manifold Σ is the x_3-axis. For any $x_0 = (0, 0, x_{30}) \in \Sigma$, we can choose $n(\phi)(x_0) = (\cos\phi, \sin\phi, 0)$, which results in

$$F^*(\phi)(x_0) = \begin{pmatrix} -\cos\phi + \frac{3}{2}\cos\phi\sin\phi + \frac{1}{2} \\ -\sin\phi + \frac{3}{2}\sin^2\phi \\ -x_{30} \end{pmatrix}, \tag{4.10}$$

$$R(\phi) = -1 + \frac{3}{2}\sin\phi + \frac{1}{2}\cos\phi, \qquad V(\phi) = -\frac{1}{2}\sin\phi. \tag{4.11}$$

The zeroes of $V(\phi)$ are $\phi_1 = 0$ and $\phi_2 = \pi$, and we have $R(0) = -1/2$ and $R(\pi) = -3/2$. That is, both $\phi_1 = 0$ and $\phi_2 = \pi$ are attracting directions. As $V'(0) < 0$ and $V'(\pi) > 0$, the direction $\phi_1 = 0$ corresponds to infinitely many ω-trajectories while $\phi_2 = \pi$ corresponds to a single ω-trajectory (see Figure 3).

Example 4.5 (system with attracting and repelling directions). Consider the system

$$F(x) = \begin{pmatrix} -\frac{x_1}{\sqrt{x_1^2+x_2^2}} + \frac{2 \cdot x_1^2}{x^2+x_2^2} - \frac{1}{2} \\ -\frac{x_2}{\sqrt{x_1^2+x_2^2}} \\ -x_3 \end{pmatrix} \tag{4.12}$$

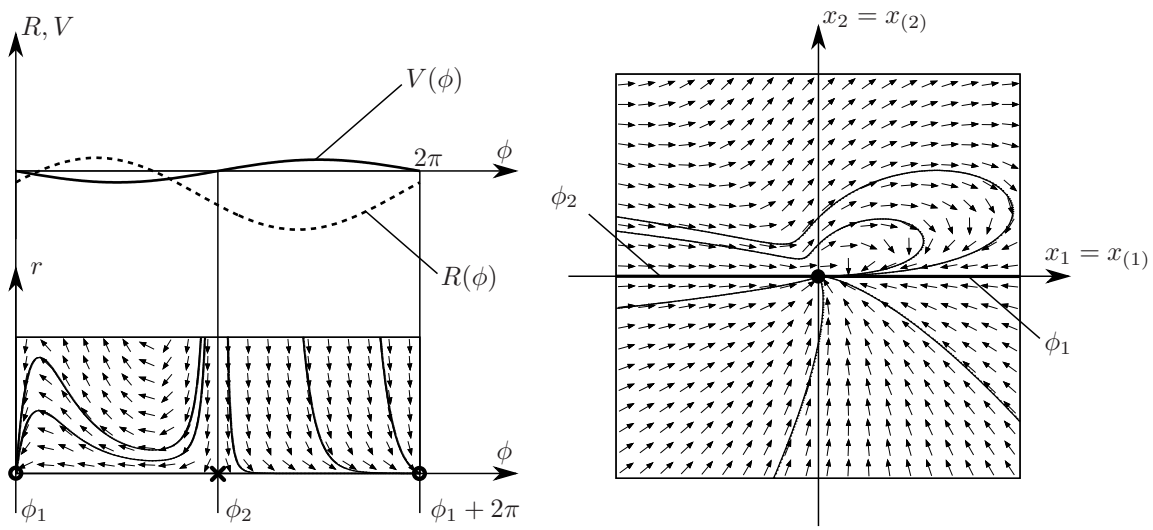

Figure 3. *Behavior of the system in Example 4.4: case of attracting directions. Top-left panel: graph of the functions $R(\phi)$ and $V(\phi)$. Bottom-left panel: projected phase portrait in polar coordinates corresponding to (4.3). The circles and crosses denote nodes and saddles, respectively. Right panel: projected phase portrait in Cartesian coordinates corresponding to (4.1). The dot denotes the point x_0 of the discontinuity set and the thick lines denote the limit directions. The depicted typical trajectories are the same in the two phase portraits.*

with $(x_1, x_2, x_3) \in \mathcal{D} = \mathbb{R}^3 \setminus \Sigma$, where the discontinuity manifold Σ is the x_3-axis, again. For any $x_0 = (0, 0, x_{30}) \in \Sigma$, we can chose $n(\phi)(x_0) = (\cos\phi, \sin\phi, 0)$, which results in

$$F^*(\phi)(x_0) = \begin{pmatrix} -\cos\phi + 2\cos^2\phi - \frac{1}{2} \\ -\sin\phi \\ -x_{30} \end{pmatrix}, \tag{4.13}$$

$$R(\phi) = -1 - \frac{1}{2}\cos\phi + 2\cos^3\phi, \qquad V(\phi) = \frac{1}{2}\sin\phi - 2\sin\phi\cos^2\phi. \tag{4.14}$$

The function $V(\phi)$ has six zeroes, $\phi_i = (i-1)\cdot\pi/3$ with $i = 1\ldots6$. The sign of $R(\phi_i)$ shows that $\phi_1 = 0$ is a repelling directions, and the other five directions are attracting. The sign of $R(\phi_i)\cdot V'(\phi)$ shows that the directions $\phi_3 = 2\pi/3$ and $\phi_5 = 4\pi/3$ are related to nodes of (4.3) and each of them corresponds to infinitely many ω-trajectories. The other directions correspond to saddles of (4.3), the direction $\phi_1 = 0$ has a single α-trajectory, and each of the directions $\phi_2 = \pi/3$, $\phi_4 = \pi$, and $\phi_6 = 5\pi/3$ has a single ω-trajectory (see Figure 4).

4.2. Case of no limit directions. Consider the case when $V(\phi) \neq 0$ for all $\phi \in [0, 2\pi)$. Then the equation $\mathrm{d}\phi/\mathrm{d}\tau = V(\phi)$ results in the fact that the solution $\phi(\tau)$ increases or decreases monotonically for all initial conditions.

Proposition 4.6. *Suppose that $V(\phi) \neq 0$ for all $\phi \in [0, 2\pi)$. Consider the quantity*

$$c_0 := \int_0^{2\pi} \frac{R(\phi)}{|V(\phi)|}\mathrm{d}\phi. \tag{4.15}$$

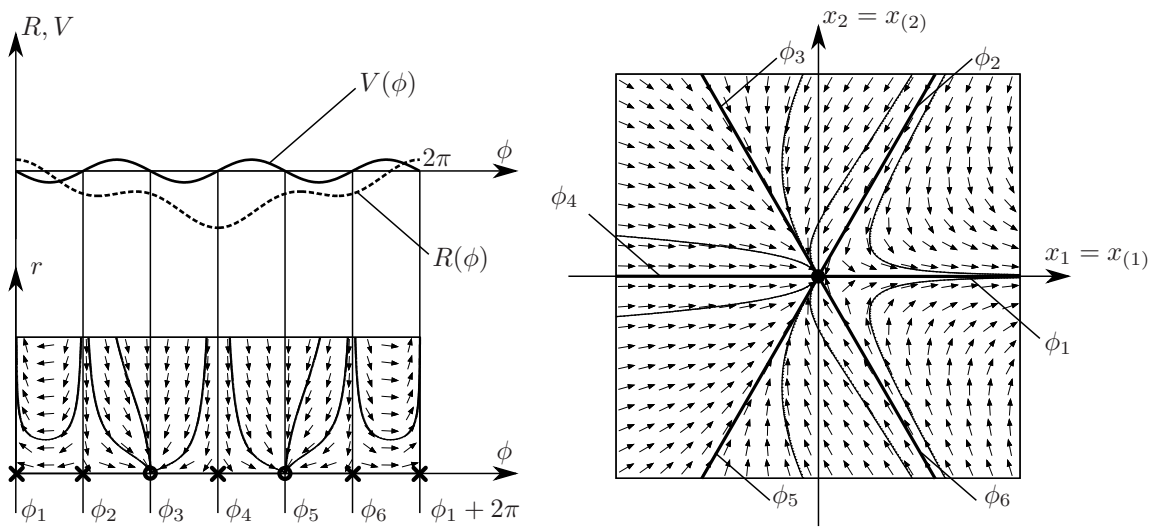

Figure 4. *Behavior of the system in Example 4.5: case of attracting and repelling directions. The notation is the same as in Figure 3. By considering the bottom-left panel, it is not clear how the trajectories between ϕ_2 and ϕ_6 can reach the repelling direction at ϕ_1. As the whole $r = 0$ axis corresponds to the origin of the original phase space, small perturbations can easily push the dynamics to the repelling direction. The internal connection(s) between the limit trajectories can be understood, e.g., by regularizing the system (see subsection 6.3).*

If $c_0 < 0$, then all trajectories of (4.5) tend to $r = 0$ in finite time in the forward direction of time. If $c_0 > 0$, then all trajectories of (4.3) tend to $r = 0$ in finite time in the backward direction of time.

Proof. Consider the initial conditions $(r, \phi) = (r_0, \phi_0)$. Then, the solution of (4.5) for r becomes

$$r(\tau) = r_0 \exp\left(\int_0^\tau R\big(\phi(s)\big)\mathrm{d}s\right). \tag{4.16}$$

If we change the variable of (4.16) from τ to ϕ, we get

$$\hat{r}(\phi) := r(\tau(\phi)) = r_0 \exp\left(\int_{\phi_0}^{\phi} \frac{R(s)}{V(s)}\mathrm{d}s\right). \tag{4.17}$$

This can be written into the form

$$\hat{r}(\phi) = r_0 \exp\left(c_1\phi\right) \cdot \exp\left(\int_{\phi_0}^{\phi} \left(\frac{R(s)}{V(s)} - c_1\right)\mathrm{d}s\right) =: r_0 \exp\left(c_1\phi\right) \cdot K(\phi), \tag{4.18}$$

where

$$c_1 := \int_0^{2\pi} \frac{R(\phi)}{V(\phi)}\mathrm{d}\phi, \qquad K(\phi) := \exp\left(\int_{\phi_0}^{\phi} \left(\frac{R(s)}{V(s)} - c_1\right)\mathrm{d}s\right) \tag{4.19}$$

and $K(\phi)$ is a periodic function with a period of 2π. The sign of the multiplier c_1 determines whether (4.18) converges to zero if $\phi \to \pm\infty$. We transform ϕ to τ and then to the original time variable t by

$$\frac{\mathrm{d}t(\phi)}{\mathrm{d}\phi} = \frac{\mathrm{d}t(\tau)}{\mathrm{d}\tau} \cdot \frac{\mathrm{d}\tau(\phi)}{\mathrm{d}\phi} = \frac{\hat{r}(\phi)}{V(\phi)}, \tag{4.20}$$

and we get

$$t(\phi) = \int_{\phi_0}^{\phi} \frac{\hat{r}(s)}{V(s)} \mathrm{d}s = \int_{\phi_0}^{\phi} \left(r_0 \exp(c_1 s) \cdot \frac{K(s)}{V(s)} \right) \mathrm{d}s. \tag{4.21}$$

As F^* is bounded and $V(\phi) \neq 0$, the sign of $V(\phi)$ is constant along $[0, 2\pi)$, which is denoted by $c_2 := \operatorname{sgn} V(\phi)$. In the case $c_1 < 0$ and $c_2 > 0$, the time for reaching $r = 0$ can be estimated by

$$0 \leq \lim_{\phi \to \infty} t(\phi) \leq \frac{r_0}{c_1 c_2} \exp(c_1 \phi_0) \cdot \max_{\phi \in [0, 2\pi)} \frac{K(\phi)}{|V(\phi)|}, \tag{4.22}$$

that is, the trajectory tends to $r = 0$ in finite time in forward direction of time. Similar estimates can be made for the different signs of c_1 and c_2. The four possibilities can be simplified to two cases by introducing the constant (4.15), which can be expressed by $c_0 = c_1 c_2$. ∎

The consequence of Proposition 4.6 is that for $c_0 < 0$, the point x_0 has infinitely many ω-trajectories and for $c_0 > 0$, the point x_0 possesses infinitely many α-trajectories. In the special case $c_1 = 0$, (4.18) becomes $\hat{r}(\phi) = r_0 K(\phi)$, which is a periodic function. Then, all solutions of (4.3) are periodic and x_0 has no limit trajectories.

We demonstrate these results on an example.

Example 4.7 (system with no limit directions). Consider the system

$$F(x) = \begin{pmatrix} \frac{x_2}{\sqrt{x_1^2+x_2^2}} - \frac{x_1/4}{\sqrt{x_1^2+x_2^2}} + \frac{1}{2} \\ -\frac{x_1}{\sqrt{x_1^2+x_2^2}} - \frac{x_2/4}{\sqrt{x_1^2+x_2^2}} \\ -x_3 \end{pmatrix} \tag{4.23}$$

with $(x_1, x_2, x_3) \in \mathcal{D} = \mathbb{R}^3 \setminus \Sigma$, where the discontinuity manifold Σ is the x_3-axis. For any $x_0 = (0, 0, x_{30}) \in \Sigma$, we can chose $n(\phi) = (\cos\phi, \sin\phi, 0)$, which leads to

$$F^*(\phi)(x_0) = \begin{pmatrix} \sin\phi - \frac{1}{4}\cos\phi + \frac{1}{2} \\ -\cos\phi - \frac{1}{4}\sin\phi \\ -x_{30} \end{pmatrix}, \tag{4.24}$$

$$R(\phi) = \frac{1}{2}\cos\phi - \frac{1}{4}, \qquad V(\phi) = -1 - \frac{1}{2}\sin\phi. \tag{4.25}$$

The function $V(\phi)$ does not have zeroes and we have $\int_0^{2\pi} R(\phi)/|V(\phi)| \mathrm{d}\phi \approx -1.814 < 0$. That is, any $x_0 \in \Sigma$ has infinitely many ω-trajectories and no α-trajectories (see Figure 5).

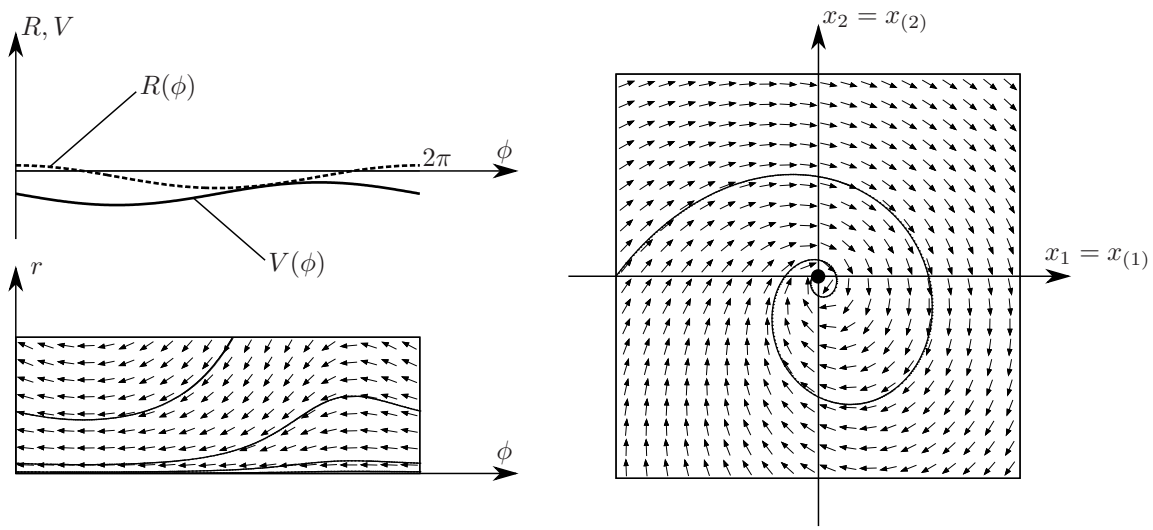

Figure 5. *Behavior of the system in Example 4.7: case of no limit directions. The notation is the same as in Figure 3. The phase portrait in Cartesian coordinates shows a focus-like behavior. However, the trajectories reach the discontinuity set in finite time.*

4.3. Effect of the different types of terms. It is important to note that all along the analysis of sections 4 and 5, the analysis is restricted to the system behavior caused by discontinuity. The systems (4.3) and (4.5) are defined by the limit vector field F^*. Therefore, they contain no information about the change of the vector field when moving away from the discontinuity manifold. It may be relevant to review the effect of neglecting of these terms from the point of view of our results.

In the vicinity of a point $x_0 \in \Sigma$, let us separate the vector field into two parts in the form

$$F(x) = F_{\text{discont}}(x) + F_{\text{cont}}(x), \tag{4.26}$$

where $F_{\text{discont}}(x)$ is defined by

$$\lim_{\epsilon \to 0^+} F_{\text{discont}}(x_0 + \epsilon n(\phi)(x_0)) - F^*(\phi)(x_0) = 0 \tag{4.27}$$

and

$$\lim_{\epsilon \to 0^+} \frac{\mathrm{d}^k F_{\text{discont}}(x_0 + \epsilon n(\phi)(x_0)}{\mathrm{d}\varepsilon^k} = 0 \tag{4.28}$$

for all $k \in \mathbb{N}^+$ and $\phi \in [0, 2\pi)$. By this construction, $F_{\text{discont}}(x)$ contains the discontinuity itself at x_0. In contrast, the continuous part $F_{\text{cont}}(x)$ contains the information about the change of the vector field when moving away from x_0. The point x_0 is a removable discontinuity of F_{cont}, because by combining (3.7), (4.26), and (4.27), we get

$$\lim_{\epsilon \to 0^+} F_{\text{cont}}(x_0 + \epsilon n(\phi)(x_0)) = 0 \tag{4.29}$$

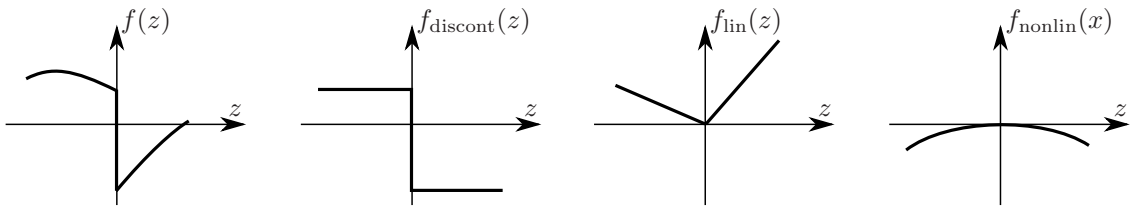

Figure 6. *Demonstration of the separation of the dynamics into continuous and discontinuous parts in the case of a simple* 1*D vector field. Consider the system* $\dot{z} = f(z)$ *with* $z \in \mathbb{R}\backslash 0$*, where the graph of* $f(z)$ *is depicted in the left panel of this figure. The vector field can be separated in the form* $f(x) = f_{\mathrm{discont}}(x)+f_{\mathrm{lin}}(x)+f_{\mathrm{nonlin}}(x)$*. In the vicinity of* $z = 0$*, the discontinuous (zero order) part has the most dominant effect on the behavior; the local structure of the dynamics is not modified by the higher order terms. A similar effect arises in the case of the extended Filippov systems in the form* (4.30).

for all $\phi \in [0, 2\pi)$. Thus, F_{cont} can be considered a continuous vector field. Note that the derivatives of F_{cont} can be still discontinuous. Formally, the vector field F_{cont} can be further separated into linear and nonlinear parts, and thus, we get

$$F(x) = F_{\mathrm{discont}}(x) + F_{\mathrm{lin}}(x - x_0) + F_{\mathrm{nonlin}}(x - x_0). \tag{4.30}$$

A similar separation of the vector field is demonstrated in case of a simple 1D vector field in Figure 6.

We want to emphasize some analogies to the fixed points of smooth vector fields. In the generic case, the structure of the dynamics in the vicinity of these fixed points is determined by the *linear part* of the system. As the linear terms typically cause exponential decay (in forward or backward time), the subexponential decay caused by the higher order (nonlinear) terms typically does not effect the local structure of the dynamics. This property of *hyperbolic* fixed points is ensured by the Hartman–Grobman theorem (see, e.g., [6, p. 61]). However, in the case of nonhyperbolic fixed points with a zero real part of an eigenvalue, the exponential decay from the linear terms vanishes (in some directions), and the structure of the dynamics is determined by the slower (subexponential) decay of the nonlinear terms.

In the case of an extended Filippov system, the effect of the discontinuity appears az a "zero order" effect, which becomes dominant even compared to the first order (linear) terms (see Table 1). As was shown in Propositions 4.3–4.6, the presence of the discontinuity typically causes decay of the trajectories *in finite time*, that is, we can consider it a stronger-than-linear (superexponential) effect. From the point of view of this zero order term F_{cont}, even the linear terms are considered higher order ones.

In this sense, the analysis of the systems (4.3) and (4.5) with neglecting the second and third terms of (4.30) is a similar process to the analysis of a fixed point of a smooth system with neglecting the nonlinear terms. If all limit directions have a definite attracting or repelling tendency ($R(\phi_i) \neq 0$; see Proposition 4.3) or there is no limit direction but a definite attracting or repelling tendency ($c_1 \neq 0$; see Proposition 4.6), then the trajectories decay to the point x_0 in finite time in forward or backward direction of the time. In this case, the relatively slow (exponential) decay of the linear terms is clearly negligible, and thus, the omitting of these terms in (4.3) and (4.5) does not modify the local structure of the dynamics.

Table 1

Speed of decay caused by the different terms in the original and transformed time scale. The time transformation (4.4) slows down the dynamics when creating (4.5) from (4.3). Then, the typical dynamics caused by the discontinuous terms becomes exponential.

Type of terms	Discont. terms (zero order)	Linear terms (first order)	Nonlinear terms (higher order)
Notation in (4.30)	F_{discont}	F_{lin}	F_{nonlin}
Original time scale (see (4.3))	superexponential	exponential	subexponential
Transformed time scale (see (4.5))	exponential	subexponential	subexponential

However, in the degenerate cases $R(\phi_i) = 0$ (in Proposition 4.3) or $c_1 = 0$ (in Proposition 4.6), there is no definite attracting or repelling behavior from the discontinuous behavior. Then, the effect of the relatively higher order (linear, nonlinear) terms should be analyzed to determine the structure of the dynamics around the chosen point x_0. Still in this case, the number and type of the limit trajectories are not affected by the linear terms because of Definitions 4.1–4.2. The connecting trajectories possibly caused by the linear and nonlinear terms are not limit trajectories in the sense of these definitions because they do not decay in finite time.

5. Sliding and crossing regions of extended Filippov systems.

In the previous section, we explored the possibilities of limit trajectories of a point $x_0 \in \Sigma$. In this section, we define sliding and crossing regions of codimension-2 discontinuity surfaces, whose definition is based on the properties of the limit trajectories.

5.1. Definition of the different regions.

5.1.1. Sliding region. It was mentioned before that the properties (a)–(c) of Proposition 2.6 are equivalent in the case of simple Filippov systems. However, these concepts are not equivalent when extending to the codimension-2 case, and thus, we have to select one of them.

The question is, Among (a)–(c), which property of the sliding region do we want to preserve when generalizing to extended Filippov systems? The most natural approach is to require that in the sliding region, a trajectory cannot be continued through the discontinuity set either in forward or in backward direction of time. Thus, roughly speaking, we can say that in the sliding region, points have either no α-trajectories or no ω-trajectories. This leads to the generalization of the property (c) of Proposition 2.6, which results in the following definition.

Definition 5.1 (sliding region in extended Filippov systems). *Consider a point $x_0 \in \Sigma$ for which we have $F^*(\phi) \notin \mathcal{T}_{x_0}\Sigma$ for all $\phi \in [0, 2\pi)$. Suppose that all limit trajectories of x_0 are either only ω-trajectories or only α-trajectories. The set of points with these properties is called the* sliding region *of Σ and denoted by $\Sigma_{sl} \subset \Sigma$. The case with ω-trajectories is called attracting sliding and the case with α-trajectories is called repelling sliding. These regions are denoted by Σ^a_{sl} and Σ^r_{sl}, respectively, and $\Sigma_{sl} = \Sigma^a_{sl} \cup \Sigma^r_{sl}$.*

From this definition, we can derive conditions to determine if a point is in the attracting or in the repelling sliding region of Σ. These propositions are not proved here as they are the direct consequences of the results of section (4).

Proposition 5.2 (condition of attracting sliding). *Consider a point $x_0 \in \Sigma$ with the functions $R(\phi)(x_0)$ and $V(\phi)(x_0)$ defined in (4.2). The point x_0 is located in the attracting sliding region Σ_{sl}^a if and only if the following statements hold:*

(a) *If there exist $\phi_i \in [0, 2\pi)$, $i = 1 \dots k$ with $V(\phi_i) = 0$, then $R(\phi_i) < 0$ for all $i = 1 \dots k$.*

(b) *If $V(\phi) \neq 0$ for all $\phi \in [0, 2\pi)$, then $\int_0^{2\pi} R(\phi)/|V(\phi)| \mathrm{d}\phi < 0$.*

In both cases, x_0 has infinitely many ω-trajectories.

Proposition 5.3 (condition of repelling sliding). *Consider a point $x_0 \in \Sigma$ with the functions $R(\phi)(x_0)$ and $V(\phi)(x_0)$ defined in (4.2). The point x_0 is located in the repelling sliding region Σ_{sl}^r if and only if the following statements hold:*

(a) *If there exist $\phi_i \in [0, 2\pi)$, $i = 1 \dots k$ with $V(\phi_i) = 0$, then $R(\phi_i) > 0$ for all $i = 1 \dots k$.*

(b) *If $V(\phi) \neq 0$ for all $\phi \in [0, 2\pi)$, then $\int_0^{2\pi} R(\phi)/|V(\phi)| \mathrm{d}\phi > 0$.*

In both cases, x_0 has infinitely many α-trajectories.

Let us apply these propositions to our previous examples. In Example 4.4, the sliding region covers the whole discontinuity set Σ. This example corresponds to case (a) of Proposition 5.2, because we can find attracting directions for the ω-trajectories. In Example 4.7, the whole discontinuity set corresponds to the sliding region, again. This example is related to case (b) of Proposition 5.2; we find no attracting directions to the ω-trajectories.

5.1.2. Crossing region. Based on the construction of Definition 5.1, we can define the crossing region for extended Filippov systems. We require that in case of crossing, any $x_0 \in \Sigma$ is connected to trajectories both in forward and backward directions of time which makes the dynamics possible to cross x_0.

Definition 5.4 (crossing region in extended Filippov systems). *Consider a point $x_0 \in \Sigma$ and suppose that x_0 possesses at least one ω-trajectory and at least one α-trajectory. The set of points with these properties is called the* crossing region *of Σ and denoted by $\Sigma_{cr} \subset \Sigma$.*

Based on the results of section 4, we can state the following proposition to determine the conditions of the crossing region.

Proposition 5.5 (condition of crossing region). *Consider a point $x_0 \in \Sigma$ with the functions $R(\phi)(x_0)$ and $V(\phi)(x_0)$ defined in (4.2). The point x_0 is located in the crossing region Σ_{cr} if and only if there exist $\phi_i \in [0, 2\pi)$, $i \in 1 \dots k$ with $V(\phi_i) = 0$ and there exist $i, j \in 1 \dots k$ for that $R(\phi_i) < 0$ and $R(\phi_j) > 0$.*

Definition 5.4 includes also the existence of several α- and ω-trajectories. In that case, the continuation of solutions through x_0 is not unique in forward or backward direction of time. In Example 4.5, all points of Σ are in the crossing region. There is only a single α-trajectory, that is, all solutions crossing x_0 leave the discontinuity set along this trajectory. However, there are infinitely many ω-directions, and hence, there is ambiguity of the solutions in the backward time direction.

5.1.3. Tangency points. The requirement $F^*(\phi) \notin \mathcal{T}_{x_0}\Sigma$ of Definition 5.1 excludes the special case when $R(\phi_i) = V(\phi_i) = 0$ for some $\phi_i \in [0, 2\pi)$. This degenerate case is defined as a tangency point. As in simple Filippov systems, tangency points are located on the boundary between sliding and crossing regions.

Definition 5.6 (tangency points in extended Filippov systems). *Consider a point $x_0 \in \Sigma$ for which there exist a $\phi_0 \in [0, 2\pi)$ with $F^*(\phi) \in \mathcal{T}_{x_0}\Sigma$. Suppose that all limit trajectories of x_0 are either only ω-trajectories or only α-trajectories. Then, the point x_0 is called a* tangency point *of Σ. The region of these points is denoted by $\Sigma_{ta} \subset \Sigma$.*

As we did for the sliding and crossing regions, properties of the tangency points can be determined from the results of section 4:

Proposition 5.7 (condition of tangency points). *Consider a point $x \in \Sigma$ with the functions $R(\phi)(x_0)$ and $V(\phi)(x_0)$ defined in (4.2). The point x_0 is located in the set Σ_{ta} of tangency points if and only if there exist $\phi_i \in [0, 2\pi)$ with $V(\phi_i) = 0$ and $i = 1 \dots k$, and the following statements hold:*

(a) *Either $R(\phi_i) \leq 0$ for all $i = 1 \dots k$ or $R(\phi_i) \geq 0$ for all $i = 1 \dots k$;*
(b) *and there exists $\phi_i \in 1 \dots k$ with $R(\phi_i) = 0$.*

Note that for $F^*(\phi) \in \mathcal{T}_{x_0}\Sigma$ for some $\phi \in [0, 2\pi)$, a point x_0 is not necessarily a tangency point. Instead, the vector field F^* can be tangent to Σ also in the crossing region. But in that case, a point $x_0 \in \Sigma$ has α- and ω- trajectories, and thus, the existence of directions with $F^*(\phi) \in \mathcal{T}_{x_0}\Sigma$ does not modify the crossing behavior. This property is different from that of the simple Filippov systems where $F^*(\phi) \in \mathcal{T}_{x_0}\Sigma$ cannot exist in the crossing region.

5.1.4. Center points. In case of simple Filippov systems, the sliding region, the crossing region, and the tangency points cover the whole discontinuity set Σ. However, in extended Filippov systems, some points are missing from these three categories. By comparing the conditions of Definitions 5.1, 5.4, and 5.6, we can realize that the case is still missing when x_0 has neither α- nor ω- trajectories. For that, a fourth region of Σ is introduced.

Definition 5.8 (center points of extended Filippov systems). *Consider a point $x_0 \in \Sigma$ for which x_0 does not have any limit trajectories. Then, the point x_0 is called a center point of Σ. The region of these points is denoted by $\Sigma_{ce} \subset \Sigma$.*

The conditions of x_0 for being a center point are the following.

Proposition 5.9 (condition of center points). *Consider a point $x_0 \in \Sigma$ with the functions $R(\phi)(x_0)$ and $V(\phi)(x_0)$ defined in (4.2). The point x_0 is located in the set Σ_{ce} if and only if the following statements hold:*

(a) *If there exist $\phi_i \in [0, 2\pi)$, $i = 1 \dots k$, with $V(\phi_i) = 0$, then $R(\phi_i) = 0$ for all $i = 1 \dots k$.*
(b) *If $V(\phi) \neq 0$ for all $\phi \in [0, 2\pi)$, then $\int_0^{2\pi} R(\phi)/|V(\phi)| \mathrm{d}\phi = 0$.*

Case (a) of Proposition 5.9 is a degenerate case which has the properties of both center points (no limit trajectories) and tangency points (boundary point between crossing and sliding regions). In case (b), center points separate the regions of attracting and repelling sliding of case (b) of Propositions 5.2 and 5.3. In the latter case, the projection F into $\mathcal{O}_{x_0}\Sigma$ results in periodic trajectories, and the phase portrait of this projected vector field is similar to a *center* of smooth systems.

Thus, we obtained a complete categorization of points of the codimension-2 discontinuity set Σ, based on the behavior of the corresponding limit trajectories. The essence of these definitions can be found in Table 2. In the next example, one can find all types of these regions of the discontinuity set.

Table 2

Classification of points of the codimension-2 discontinuity manifolds in extended Filippov systems. The table is based on the conditions of Definitions 5.1, 5.4, 5.6, and 5.8. This results in a complete categorization of the points of Σ, and we have $\Sigma_{sl} \cup \Sigma_{cr} \cup \Sigma_{ta} \cup \Sigma_{ce} = \Sigma$. The first and second columns of the sliding region correspond to attracting and repelling sliding, respectively. The first and second columns of the tangency points show whether the tangency point separates the crossing region from the attracting or repelling sliding region, respectively. All these cases can be found in Example 5.10.

Subset of Σ	Sliding region		Crossing region	Tangency points		Center points
Notation	Σ_{sl}		Σ_{cr}	Σ_{ta}		Σ_{ce}
α-trajectories	no	yes	yes	no	yes	no
ω-trajectories	yes	no	yes	yes	no	no
$F^*(\phi) \in \mathcal{T}_{x_0}\Sigma$	no		yes or no	yes		yes or no

Example 5.10 (system with all typical behaviors). Consider the system

$$F(x) = \begin{pmatrix} \frac{x_4x_1 - x_3x_2}{\sqrt{x_1^2+x_2^2}} + 1 \\ \frac{x_4x_2 + x_3x_1}{\sqrt{x_1^2+x_2^2}} \\ -x_3 \\ -x_4 \end{pmatrix} \tag{5.1}$$

with $x = (x_1, x_2, x_3, x_4) \in \mathcal{D} = \mathbb{R}^4 \setminus \Sigma$, where the discontinuity manifold Σ is the $x_3 - x_4$-plane. For any $x_0 = (0, 0, x_{30}, x_{40}) \in \Sigma$, we can choose $n(\phi)(x_0) = (\cos\phi, \sin\phi, 0, 0)$, which results in

$$F^*(\phi)(x_0) = \begin{pmatrix} x_{40}\cos\phi - x_{30}\sin\phi + 1 \\ x_{40}\sin\phi + x_{30}\cos\phi \\ -x_{30} \\ -x_{40} \end{pmatrix}, \tag{5.2}$$

$$R(\phi) = x_{40} + \cos\phi, \qquad V(\phi) = x_{30} - \sin\phi. \tag{5.3}$$

The behavior of the trajectories in the vicinity of x_0 can be visualized in the discontinuity surface Σ, which is the plane of the variables x_3 and x_4 (see Figure 7). The lines $x_3 = \pm 1$ separate the cases when $V(\phi)$ has or does not have zeroes. If $V(\phi)$ has zeroes, then the circle $x_3^2 + x_4^2 = 1$ gives the location of the tangency points, whose curve separates the sliding and crossing regions. If $V(\phi)$ does not have zeroes, then the center points are located on the line $x_4 = 0$, and this line separates the domains of attracting and repelling regions.

5.2. Necessary condition of sliding region. In this subsection, we prove Theorem 5.11, which provides a necessary condition for sliding which can be checked by using a single formula. On the other hand, this theorem will be used to prove Theorem 5.15.

The projection (4.1) of the limit vector $F^*(\phi)$ into the orthogonal space $\mathcal{O}_{x_0}\Sigma$ can be formulated as a complex function

$$F_c^*(\phi) = F_{(1)}(\phi) + \mathrm{i} \cdot F_{(2)}(\phi), \tag{5.4}$$

where the notation i is used for the imaginary unit in this subsection only. The graph of F_c^* is a closed curve in the complex plane.

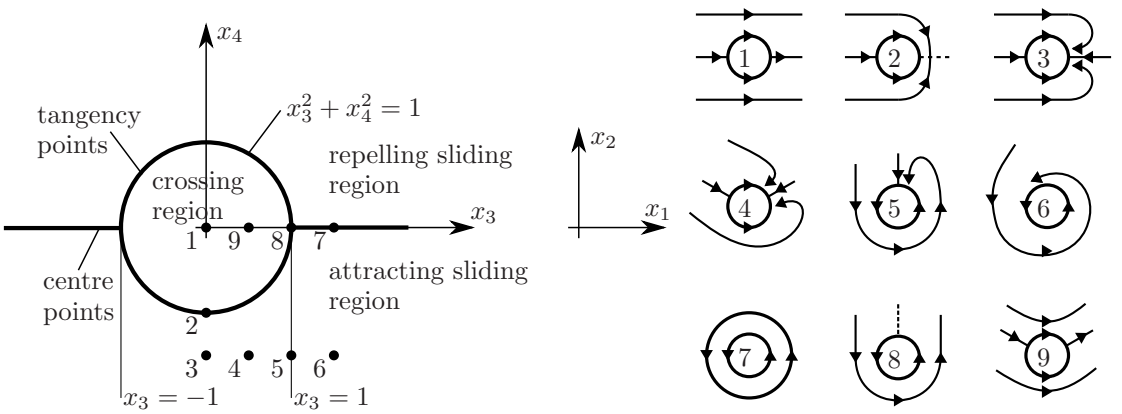

Case	1	2	3	4	5	6	7	8	9
Behavior	Crossing	Tangency	Sliding				Center		Crossing
Number of saddles	2	1	1	1	0	0	0	0	2
Number of stable nodes	0	0	1	1	0	0	0	0	0
No. of degenerate fixed points	0	1	0	0	1	0	0	1	0

Figure 7. *Behavior of the system in Example 5.10. Left panel: sketch of the discontinuity set $x_1 = x_2 = 0$ with the different regions. In the right panel, the typical trajectories are visualized in the orthogonal space spanned by x_1 and x_2. The numbers corresponds to the points shown in the left panel. As in Figures 3–5, the trajectories are projected into the orthogonal space. The origin is blown up to a small circle to better understanding of the trajectories. The cases numbered by 1–9 are listed in the table with the corresponding behavior (crossing, sliding, tangency, center) and the number and type of the fixed points on the blowup circle.*

If $F^*(\phi_j) \in \mathcal{T}_{x_0}\Sigma$ for some $\phi_j \in [0, 2\pi)$, then $F_c^*(\phi_j) = 0$, that is, F_c^* crosses the origin. If $F^*(\phi) \neq 0$ for all $\phi \in [0, 2\pi)$, then Cauchy's argument principle can be applied in the form

$$N := \frac{\arg F_c^*(2\pi) - \arg F_c^*(0)}{2\pi} = \frac{1}{2\pi i}\int_0^{2\pi} \frac{F_c'(\phi)}{F_c(\phi)}\mathrm{d}\phi \tag{5.5}$$

to calculate the number $N \in \mathbb{N}$ of encirclements of F_c^* around the origin. By expressing F_c^* by the functions R and V, (5.5) becomes

$$N = 1 + \frac{1}{2\pi}\int_0^{2\pi} \frac{R(\phi)V'(\phi) - V(\phi)R'(\phi)}{R^2(\phi) + V^2(\phi)}\mathrm{d}\phi. \tag{5.6}$$

The unit normal vectors $n(\phi)$ can be defined also in complex form by

$$n_c(\phi) := \langle n(\phi), n_{(1)}\rangle + \mathrm{i}\cdot\langle n(\phi), n_{(2)}\rangle = \cos\phi + \mathrm{i}\cdot\sin\phi. \tag{5.7}$$

Let us define the function

$$\gamma(\phi) := \arg F_c^*(\phi) - \arg n_c(\phi) = \arg F_c^*(\phi) - \phi, \tag{5.8}$$

which expresses the angle between $F_c^*(\phi)$ and $n_c(\phi)$ in the complex plane. The multivalued arg function makes the definition of γ ambiguous, but by prescribing $\gamma(0) \in [0, 2\pi)$ and by

requiring γ to be continuous, (5.8) becomes completely defined. Then, the difference

$$\gamma(2\pi) - \gamma(0) = \arg F_c^*(2\pi) - \arg F_c^*(0) - 2\pi = 2\pi(N-1) \tag{5.9}$$

can be expressed by the number N of encirclements from (5.6).

It can be shown by direct calculation that the values ϕ_j with $\gamma(\phi_j) = 2n\pi$ and $n \in \mathbb{N}$ are the repelling directions of x_0. Similarly, $\gamma(\phi_j) = (2n+1)\pi$ corresponds to the attracting directions. This leads to the following theorem.

Theorem 5.11 (necessary condition for existence of sliding). *If point $x_0 \in \Sigma$ is located in the sliding region Σ_{sl}, then the number N of encirclements of F_c^* around the origin is 1, that is,*

$$\int_0^{2\pi} \frac{R(\phi)V'(\phi) - V(\phi)R'(\phi)}{R^2(\phi) + V^2(\phi)} \mathrm{d}\phi = 0. \tag{5.10}$$

Proof. From (5.6), the condition (5.10) is equivalent to $N = 1$, and from (5.9), this is equivalent to $\gamma(2\pi) = \gamma(0)$. If $N \neq 1$, then $\gamma(2\pi) = \gamma(0) + 2\pi K$ with $K = N - 1$. Hence, there exists an integer n for that both $2n\pi$ and $(2n+1)\pi$ are in $[\gamma(0), \gamma(2\pi)]$ or in $[\gamma(2\pi), \gamma(0)]$. Then, the intermediate value theorem guarantees that the function γ takes both values. That is, there is an attracting and a repelling direction, and thus, x_0 is in the crossing region. ∎

Note that the converse of Theorem 5.11 is not true and $N = 1$ does not guarantee the sliding behavior. For instance, consider $R(\phi) = \cos\phi - \sin(\phi)/2$ and $V(\phi) = \sin(2\phi)$. In this case, we have $N = 1$ but there are two attracting and two repelling directions which means crossing behavior.

5.3. Sliding dynamics.

5.3.1. Construction of the sliding dynamics.

Let us present a natural generalization of the convex combination to extended Filippov systems to construct the sliding vector field F_s. Analogously to (2.13), the convex combination of the vectors of the limit vector field $F^*(\phi)$ can be written in the form

$$F_s = \int_0^{2\pi} \alpha(\phi) \cdot F^*(\phi)\, \mathrm{d}\phi, \tag{5.11}$$

where the α is a $[0, 2\pi) \to \mathbb{R}$ function with

$$\int_0^{2\pi} \alpha(\phi)\, \mathrm{d}\phi = 1. \tag{5.12}$$

Instead of the discrete weights α_1 and α_2 of simple Filippov systems, we have now a weight *function* $\alpha(\phi)$ on the domain $[0, 2\pi)$. The convex combination requires $\alpha(\phi) \geq 0$ for all $\phi \in [0, 2\pi)$. The convex combination is *trivial* if $F_s = F^*(\phi_1)$ for some $\phi_1 \in [0, 2\pi)$, which results in $\alpha(\phi) = \delta(\phi - \phi_1)$, where δ is the Dirac delta function. To exclude this case, we can define the *nontrivial* convex combination when we have $\phi_1 \neq \phi_2$ for which $\alpha(\phi_1), \alpha(\phi_2) > 0$.

Analogously to (2.14), the sliding vector field can be written also in the form

$$F_s = \overline{F} + \frac{1}{2\pi} \int_0^{2\pi} \beta(\phi) \left(F^*(\phi) - \overline{F}\right) \mathrm{d}\phi, \tag{5.13}$$

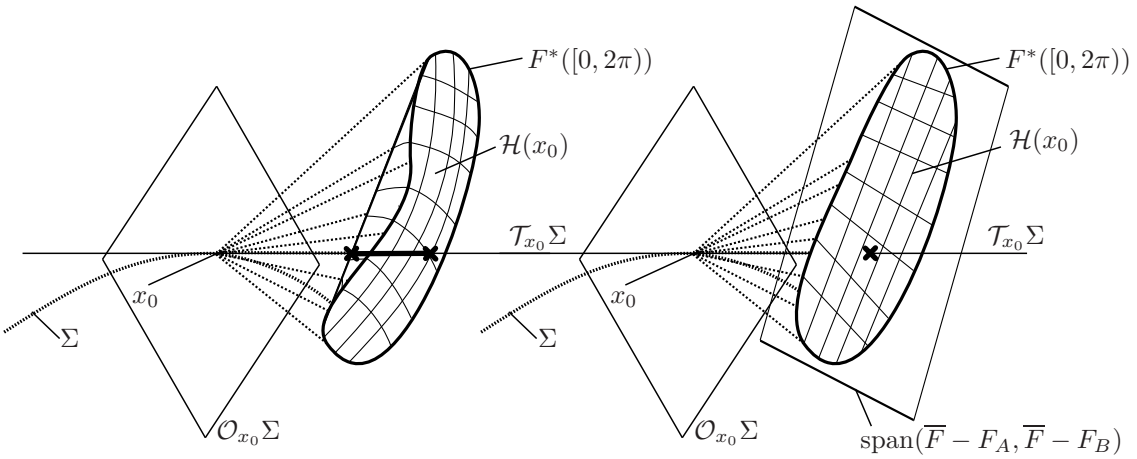

Figure 8. *Uniqueness of the sliding vector of extended Filippov systems. Left panel: in the general case, the convex hull $\mathcal{H}(x_0)$ of $F^*([0,2\pi))$ is an m dimensional body. Its intersection with the tangent space $\mathcal{T}_{x_0}\Sigma$ results in an $m-2$ dimensional set of the possible sliding vectors (thick line between the crosses). Right panel: if the limit vector field has a form of (5.16), then the convex hull lays in a 2D hyperplane and the intersection provides a unique sliding vector (denoted by a cross).*

where

$$\overline{F} := \frac{1}{2\pi}\int_0^{2\pi} F^*(\phi)\mathrm{d}\phi \tag{5.14}$$

is the integral average of F^* on $[0,2\pi)$, and β is a $[0,2\pi)\to\mathbb{R}$ function with

$$\frac{1}{2\pi}\int_0^{2\pi} \beta(\phi)\mathrm{d}\phi = 0. \tag{5.15}$$

By comparing (5.11) and (5.13), we get $\beta(\phi) = 2\pi\alpha(\phi) - 1$. Thus, for the convex combination, we require $\beta(\phi) \geq -1$ for all $\phi \in [0,2\pi)$. In the case of nontrivial convex combination, there exist $\phi_1 \neq \phi_2$ for which $\beta(\phi_1), \beta(\phi_2) > -1$.

We require that the resulting sliding vector F_s is tangent to Σ, that is, $F_s \in \mathcal{T}_{x_0}\Sigma$. The existence and the uniqueness of such F_s is determined by the set $\mathcal{T}_{x_0}\Sigma \cap \mathcal{H}(x_0)$, where $\mathcal{H}(x_0)$ is the convex hull of the set $F^*([0,2\pi))$. The sliding vector F_s exists if $\mathcal{T}_{x_0}\Sigma \cap \mathcal{H}(x_0)$ is nonempty. A sufficient condition for existence is provided by Theorem 5.15.

The sliding vector F_s is unique if $\mathcal{T}_{x_0}\Sigma \cap \mathcal{H}(x_0)$ contains a single element, which is not satisfied in general (see Figure 8). The set $\mathcal{H}(x_0)$ is a convex m dimensional set and $\mathcal{T}_{x_0}\Sigma$ is an $m-2$ dimensional subspace of $\mathbb{R}^m$. In the general case of a nonempty $\mathcal{T}_{x_0}\Sigma \cap \mathcal{H}(x_0)$, the intersection is an $m-2$ dimensional subset of $\mathcal{T}_{x_0}\Sigma$, which contains continuously many suitable sliding vectors. This property is similar to the systems with intersection of n codimension-1 discontinuity manifolds [15]. In that case, Jeffrey suggests a natural choice of the sliding vector by constructing the *convex canopy* of the 2^{n+1} limit vectors. It is an open question if there is a similar natural choice of F_s in the case of isolated codimension-2 discontinuity sets. A necessary condition for uniqueness is presented in subsection 5.3.2.

5.3.2. Necessary condition for uniqueness of sliding. To ensure a unique nontrivial sliding vector, we require the convex hull $\mathcal{H}(x_0)$ to be two dimensional. This special case occurs often at mechanical problems with Coulomb friction. (See the examples in section 6.) The set $\mathcal{H}(x_0)$ is 2D if the curve $F^*([0,2\pi))$ lays in a 2D hyperplane in $\mathbb{R}^m$.

Theorem 5.12 (necessary condition for uniqueness of sliding). *Suppose that F^* can be written in the form*

$$F^*(\phi) = \overline{F} + A(\phi)\cdot F_A + B(\phi)\cdot F_B, \tag{5.16}$$

where F_A, F_B are vectors in $\mathbb{R}^m$, and $\operatorname{span}(\overline{F}-F_A, \overline{F}-F_B)$ is not parallel to $\mathcal{T}_{x_0}\Sigma$. The vector $\overline{F}$ is the integral average defined in (5.14), and $A(\phi), B(\phi)$ are $[0,2\pi)\to\mathbb{R}$ functions with

$$\int_0^{2\pi} A(\phi)\mathrm{d}\phi = 0, \qquad \int_0^{2\pi} B(\phi)\mathrm{d}\phi = 0. \tag{5.17}$$

In that case, (5.11) provides a unique sliding vector $F_s \in \mathcal{T}_{x_0}\Sigma$.

Proof. Substituting (5.16) into (5.11) results in

$$F_s = \overline{F} + \int_0^{2\pi} \alpha(\phi)A(\phi)\mathrm{d}\phi\cdot F_A + \int_0^{2\pi} \alpha(\phi)B(\phi)\mathrm{d}\phi\cdot F_B = \overline{F} + a\,F_A + b\,F_B, \tag{5.18}$$

where

$$a := \int_0^{2\pi} \alpha(\phi)A(\phi)\mathrm{d}\phi, \qquad b := \int_0^{2\pi} \alpha(\phi)B(\phi)\mathrm{d}\phi. \tag{5.19}$$

The condition $F_s \in \mathcal{T}_{x_0}\Sigma$ is equivalent to the conditions $\langle F_s, n_{(1)}\rangle = 0$ and $\langle F_s, n_{(2)}\rangle = 0$, where $n_{(1)}$ and $n_{(2)}$ are the basis vectors of $\mathcal{O}_{x_0}\Sigma$. These conditions lead to

$$\begin{aligned} \langle \overline{F}, n_{(1)}\rangle + \langle F_A, n_{(1)}\rangle \cdot a + \langle F_B, n_{(1)}\rangle \cdot b = 0,\\ \langle \overline{F}, n_{(2)}\rangle + \langle F_A, n_{(2)}\rangle \cdot a + \langle F_B, n_{(2)}\rangle \cdot b = 0. \end{aligned} \tag{5.20}$$

As $\operatorname{span}(\overline{F}-F_A, \overline{F}-F_B)$ is not parallel to $\mathcal{T}_{x_0}\Sigma$, (5.20) is independent, and thus, there is unique solution for a and b, and then, (5.18) gives an unique F_s. ∎

Note that the theorem does not guarantee the existence of such F_s that is constructed as a *convex* combination of F^*. The existence of sliding also requires a weight function α with $\alpha(\phi) \geq 0$. The unique values a and b still not determine a unique weight function $\alpha(\phi)$, but (5.19) determines a class of possible weight functions. Thus, the direct checking of $\alpha(\phi) \geq 0$ is not straightforward. Instead, one can use the sufficient condition for existence provided by Theorem 5.15, which states that there always exists a sliding vector in the sliding region.

5.4. Comparison with possible alternative definitions of sliding region. We decided to preserve the property (c) of Proposition 2.6 when extending the definition of sliding region to extended Filippov systems. It would be also possible to extend the properties (a) and (b), which would result in different definitions of the sliding region.

5.4.1. Comparison with the definition from the radial dynamics. The property (a) of Proposition 2.6 means that the component of the limit vector field F^* in the direction of the

corresponding normal vector n points toward the discontinuity set. The natural extension of this property leads to the following definition.

Definition 5.13 (region with attracting or repelling radial dynamics). *Consider a point $x_0 \in \Sigma$ with the function $R(\phi)(x_0) = \langle F^*, n\rangle(\phi)(x_0)$. Suppose that either $R(\phi) < 0$ for all $\phi \in [0, 2\pi)$ or $R(\phi) > 0$ for all $\phi \in [0, 2\pi)$. The set of such points are denoted by $\Sigma_{radial} \subset \Sigma$.*

The sliding region of Filippov systems is usually defined by Definition 2.1, and therefore, it seems to be natural to extend the concept of sliding region by Definition 5.13. The authors also suggested this definition in [3], because Definitions 5.1 and 5.13 give the same results in many mechanical examples with Coulomb friction. However, analysis of the present paper shows that Definition 5.13 would result in a *too strong* definition of sliding region.

It is obvious that $\Sigma_{radial} \subset \Sigma_{sl}$, because the constant sign of R is valid also for the limit directions. However, there are points in the sliding region Σ_{sl} which are not located in Σ_{radial}. In Example 4.4, the function $R(\phi)$ changes sign along $[0, 2\pi)$, that is, $x_0 \notin \Sigma_{radial}$. However, the directions ϕ_i of the limit trajectories are both located in the subset of $[0, 2\pi)$ with $R(\phi) < 0$, which results in an attracting sliding behavior. In Example 4.7, $R(\phi)$ also changes sign along $[0, 2\pi)$, but the integral (4.15) shows that all limit trajectories of x_0 are ω-trajectories, and x_0 is located in the sliding region.

A further disadvantage of Definition 5.13 is that smooth transformation of the variables could change the radially attracting or repelling property of the system. In Definitions 5.1 and 5.4, such coordinate transformation cannot change the sliding or crossing property.

5.4.2. Comparison with the definition from existing sliding vector. The sliding region could also be defined from the extension of property (b) of Proposition 2.6, which requires the existence of the sliding vector constructed from convex combination. In the case of extended Filippov systems, this condition leads to the following definition.

Definition 5.14 (region with sliding vector from convex combination). *Consider a point $x \in \Sigma$ and suppose that there exists a sliding vector $F_s \in \mathcal{T}_{x_0}\Sigma$, where (5.11) is a nontrivial convex combination. The set of such points are denoted by $\Sigma_{convex} \subset \Sigma$.*

In other words, Σ_{convex} contains the points x_0 such that the intersection $\mathcal{T}_{x_0}\Sigma \cup \mathcal{H}(x_0)$ is nonempty. The relation between Σ_{convex} and the sliding region Σ_{sl} is given by the following theorem.

Theorem 5.15 (existence of the sliding vector in the sliding region). *If x_0 is located in the sliding region Σ_{sl}, then there exists a sliding vector $F_s \in \mathcal{T}_{x_0}\Sigma$, where (5.11) is a nontrivial convex combination. That is, $\Sigma_{sl} \subset \Sigma_{convex}$.*

Proof. Theorem 5.11 states that in the sliding region, the graph of projection of F^* into $\mathcal{O}_{x_0}\Sigma$ circles around the origin once. That is, the origin is in the interior of the convex hull of $F_c^*([0, 2\pi))$. By projection to $\mathcal{O}_{x_0}\Sigma$, the origin is the image of all points of $\mathcal{T}_{x_0}\Sigma$ and $F_c^*([0, 2\pi))$ is the image of $F^*([0, 2\pi))$. Therefore, $F^*([0, 2\pi)) \cap \mathcal{T}_{x_0}\Sigma$ is nonempty, and $x_0 \in \Sigma_{convex}$. ∎

The converse of Theorem 5.15 is not true; a point $x_0 \in \Sigma_{convex}$ with an existing sliding vector is not necessarily located in the sliding region. In Example 4.5, the sliding vector $F_s = (0, 0, -x_{30})$ can be constructed as a nontrivial convex combination of $F^*(\phi)$ for all

$(0, 0, x_{30}) \in \Sigma$. However, the whole discontinuity set corresponds to the crossing region. That is, Definition 5.14 would result a *too weak* definition for sliding region.

In this subsection, we showed that the extension of the properties of Proposition 2.6 lead to different subsets of the discontinuity set Σ, determined by Definitions 5.1, 5.13, and 5.14. Among them, we chose Definition 5.1 because it seems to be the most natural extension of the sliding region of simple Filippov systems to the extended Filippov systems. Definition 5.13 provides a sufficient condition and Definition 5.14 gives a necessary condition for sliding behavior.

6. Application to mechanical systems with Coulomb friction. The motivation behind developing the mathematical methods in this paper was the mechanical problems with Coulomb friction in three dimensions.

Consider two rigid bodies slipping on each other at a single contact point, and assume a simple Coulomb model where the magnitude of the friction force is proportional to the normal force and its direction is opposite to the relative velocity at the contact point. Then, the components C_1 and C_2 of the friction force can be written into the form

$$C_1 = -\mu N \frac{u_1}{\sqrt{u_1^2 + u_2^2}}, \qquad C_2 = -\mu N \frac{u_2}{\sqrt{u_1^2 + u_2^2}}, \tag{6.1}$$

where N is the normal force between the bodies, μ is the friction coefficient, and u_1, u_2 are the components of the relative velocity in the tangent plane at the contact point in the same coordinate system used for C_1 and C_2. In the special planar (2D) case with $u_2 \equiv 0$, (6.1) leads to

$$C_1 = -\mu N \frac{u_1}{|u_1|}, \qquad C_2 = 0. \tag{6.2}$$

In the derivation of the differential equations of the rigid bodies from the Newton–Euler equations, the expression of the accelerations leads to the solution of a linear algebraic equation. Thus, the discontinuous terms $u_1/|u_1|$ and $u_1/\sqrt{u_1^2 + u_2^2}$ appears in the resulting differential equations, as well. In the planar case, the discontinuity at $u_1 = 0$ is a codimension-1 discontinuity manifold, and thus, it leads to a simple Filippov system. In the spatial (3D) case, $u_1 = u_2 = 0$ is a codimension-2 discontinuity manifold, and thus, it leads to an extended Filippov system.

The classical method to analyze these mechanical systems is to derive the equations of motion separately for the case of the rolling of the bodies. At the discontinuity of the slipping equations, the dynamics is replaced by the rolling equations. This approach can be used for the numerical simulation of the system (see, e.g., [22]), but it gives not much information of the connection between the rolling and slipping behavior. The theory of Filippov systems provide a deeper understanding of the problem by analyzing the discontinuous behavior of the vector field. The theory of simple Filippov systems can be used effectively for systems with planar Coulomb friction (see the examples and applications in [6]), but not in the 3D case. However, extended Filippov systems can be used for the analysis of systems with spatial Coulomb friction between 3D rigid bodies.

In this section, we demonstrate the methods presented above on two mechanical examples. In these examples, we determine the dynamical equations by the Newton–Euler equations in the spatial case which provide an extended Filippov system. From the vector field F, the

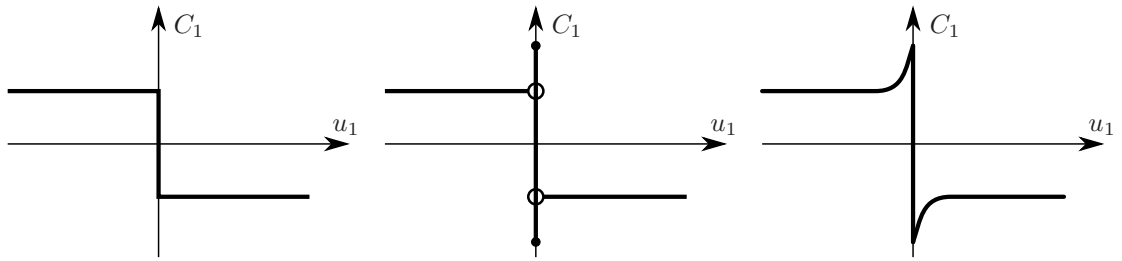

Figure 9. *Different types of Coulomb model given by the relation between the friction force C_1 and the slipping velocity u_1. These diagrams refer to the planar (2D) case (see (6.2)), but similar (multivariable) models are used in the spatial (3D) case. Left panel: simple Coulomb model with no difference between static and dynamic friction. Middle panel: sticktion model with discontinuity between the static and dynamic friction. In this case, the convex methods of both simple Filippov systems and extended Filippov systems do not give a proper result. Right panel: Coulomb friction and Stribeck effect with continuous connection between static and dynamic friction. In this case, convex methods can be applied again, both in simple Filippov systems and extended Filippov systems.*

sliding region and the sliding dynamics can be determined based on the definitions above. We find that the sliding dynamics is the same that one could get from applying Newton's second law *separately* for the nonslipping (sticking or rolling) case. Moreover, the condition of being in the sliding region becomes the same as the condition of the maximal possible static friction in case of the Coulomb model. Thus, methods of extended Filippov systems can be used in problems with spatial Coulomb friction in the same way as using simple Filippov systems for planar Coulomb friction.

In the following examples, we assume simple Coulomb friction with uniform magnitude of static and dynamic friction force. (See the left panel of Figure 9.) As in the case of simple Filippov systems, the convex methods of extended Filippov systems do not work automatically with the *sticktion* model where the independent values of static and dynamic friction introduce an additional discontinuity to the model. (See the middle panel of Figure 9.) However, the methods work again if the Stribeck-effect is also considered. (See the right panel of Figure 9.)

In the examples below, we do not just reproduce those results obtained from considering the sticking or rolling dynamics, but we can get additional information about the limit trajectories, as well; which describes the qualitative behavior of the system at slipping-rolling or slipping-sticking transitions. Moreover, the presented methods can be applied to determine the condition of slipping even in some cases where this process cannot be carried out by checking the maximal friction force (see [1] and [2]). The application of extended Filippov systems has similarities to the method used in [4] for mechanical systems with friction between colliding bodies.

6.1. Rigidly connected pair of mass points on the plane. Let us consider a rigid body on a horizontal plane which consist of two mass points P and Q connected by a rigid massless rod (see Figure 10). The mass points have uniform mass m, the length of the rod is $2d$. The mass point P is subjected to Coulomb friction with a friction coefficient μ; the friction between the mass point Q and the plane is neglected. A torque T is acting on the body in the vertical direction. The gravitational acceleration is denoted by g.

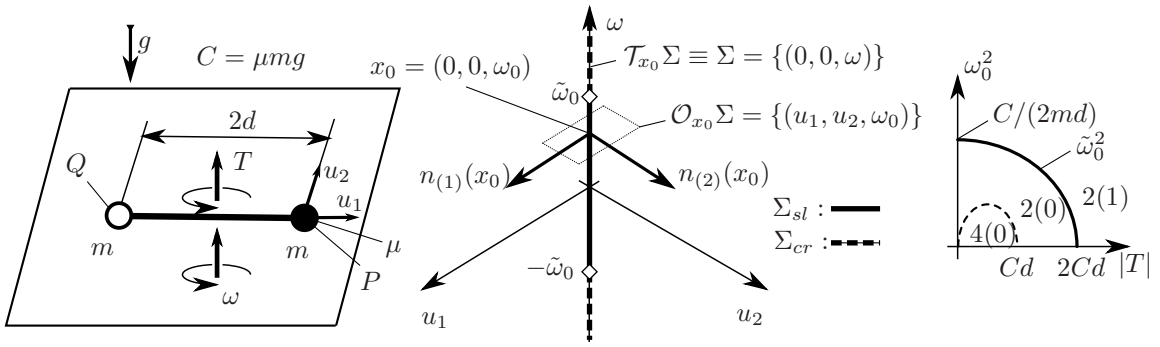

Figure 10. *Rigidly connected pair of mass points on the plane. Left panel: sketch of the mechanical model with the parameters and state variables. Middle panel: sketch of the state space in the case $|T| \leq 2Cd$. Then, there are two tangency points at $\pm\tilde{\omega}_0$. Between the tangency points, there is sliding (thick solid line), and outside, there is crossing (thick dashed line). Right panel: location $\tilde{\omega}_0$ of the tangency points as a function of the moment M. The numbers in the form $N(M)$ in the different regions of the graph denote that the number of limit directions is N, and M of them are repelling directions.*

6.1.1. Dynamics. In this mechanical system, the location and the orientation do not modify the dynamics, and the state of the body can be described by the velocity state only. Let $x = (u_1, u_2, \omega)$, where ω is the angular velocity of the body, while u_1 and u_2 are the velocity components of the mass point P described in a coordinate system attached to the body. (See the left panel of Figure 10.) By assuming that P is slipping on the plane, the relevant components of the Newton–Euler equations are

$$\begin{aligned} 2m \cdot \left(\dot{u}_1 - \omega u_2 + \omega^2 d\right) &= C_1, \\ 2m \cdot \left(\dot{u}_2 - \dot{\omega} d\right) &= C_2, \\ 2md^2\dot{\omega} &= C_2 d + T, \end{aligned} \tag{6.3}$$

where

$$C_1 = -\mu m g \frac{u_1}{\sqrt{u_1^2 + u_2^2}}, \qquad C_2 = -\mu m g \frac{u_2}{\sqrt{u_1^2 + u_2^2}} \tag{6.4}$$

are the components of the Coulomb friction force at the mass point P. The first two equations of (6.3) are the two components of Newton's second law in the horizontal plane, where the expressions in the brackets are the acceleration components of the center of the gravity of the body. Note that the velocities u_1 and u_2 are measured in the inertial (fixed) reference system but in a coordinate system *co-rotating* with the body, which leads to additional terms in the accelerations. The third component of (6.3) is the Euler equation of rotation for the vertical direction. From (6.3), the time derivatives of the variables can be expressed, and we get the differential equation

$$\begin{pmatrix} \dot{u}_1 \\ \dot{u}_2 \\ \dot{\omega} \end{pmatrix} = F(x) = \begin{pmatrix} -\frac{C}{2m}\frac{u_1}{\sqrt{u_1^2+u_2^2}} + \omega u_2 - \omega^2 d \\ -\frac{C}{m}\frac{u_2}{\sqrt{u_1^2+u_2^2}} - \omega u_1 + \frac{T}{2md} \\ -\frac{C}{2md}\frac{u_2}{\sqrt{u_1^2+u_2^2}} + \frac{T}{2md^2} \end{pmatrix}, \tag{6.5}$$

where $C := \sqrt{C_1^2 + C_2^2} = \mu m g$ is the magnitude of the Coulomb friction force at slipping. Note that the velocities u_1 and u_2 are not interchangeable in (6.5) because these variables are measured in the rotating coordinate system connected to the body. For example, an additional 2 in the denominator appears in the first component of (6.5); a unit force *acting at* P can create half of the acceleration in the direction u_1 (when accelerating both mass points) than in the direction of u_2 (when only one of them is accelerated due to the rotation of the body).

The discontinuity set Σ is the line determined by $u_1 = u_2 = 0$; this corresponds to the case when the point P is stuck to the plane. For any $x_0 = (0, 0, \omega_0) \in \Sigma$, we can choose the basis vectors $n_{(1)} = (1, 0, 0)$, $n_{(2)} = (0, 1, 0)$. Then, the limit vector field becomes

$$F^*(\phi)(x_0) = \begin{pmatrix} -\frac{C}{2m}\cos\phi - \omega_0^2 d \\ -\frac{C}{m}\sin\phi + \frac{T}{2md} \\ -\frac{C}{md}\sin\phi + \frac{T}{2md^2} \end{pmatrix}. \tag{6.6}$$

The physical meaning of ϕ is the direction of slipping of point P on the plane.

6.1.2. Sliding and crossing regions. Let us now determine the sliding and crossing regions of the system. From (6.6), we get

$$R(\phi) = -\frac{C}{2m}\left(1 + \sin^2\phi\right) - \omega_0^2 d\cos\phi + \frac{T}{2md}\sin\phi, \tag{6.7}$$

$$V(\phi) = -\frac{C}{2m}\cos^2\phi + \omega_0^2 d\sin\phi + \frac{T}{2md}\cos\phi. \tag{6.8}$$

Determining the zeroes of (6.7) leads to a fourth order polynomial in $\cos\phi$, which results in lengthy formulae. Instead, let us determine the special case of tangency points which separate the sliding and crossing behavior. The necessary condition of the tangency points is to have a direction ϕ_1 with $V(\phi_1) = R(\phi_1) = 0$, which results in

$$\sin\phi_1 = \frac{T}{2dC}, \qquad \cos\phi_1 = -\sqrt{1 - \left(\frac{T}{2dC}\right)^2}, \qquad \tilde{\omega}_0^2 = \sqrt{\left(\frac{C}{2md}\right)^2 - \left(\frac{T}{4md^2}\right)^2}. \tag{6.9}$$

That is, the tangency points are located at $\omega = \pm\tilde{\omega}_0$ (see Figure 10), and then, the direction ϕ_1 on the boundary of being an attracting or a repelling direction is determined by (6.9). It can be checked that in that case, the direction $\phi_2 = \pi - \phi_1$ is always an attracting direction and there are no other limit directions. It can be shown that the case $|\omega_0| < \tilde{\omega}_0$ corresponds to the attracting sliding region and the case $|\omega_0| > \tilde{\omega}_0$ corresponds to the crossing region. The tangency points exist only if $|T| \le 2dC$; otherwise, the crossing region covers all the discontinuity set Σ. (See the right panel of Figure 10.) This is consistent to the results from the assumption of the the maximal admissible friction force at the Coulomb model.

The special case $\omega_0 = 0$ can still be investigated analytically. Then, we get

$$V(\phi) = \cos\phi\left(-\frac{C}{2m}\cos\phi + \frac{T}{2md}\right). \tag{6.10}$$

In the case $|T| < dC$, there are four attracting directions (sliding), in the case $dC \le |T| \le 2dC$, there are two attracting directions (still sliding), and in the case $|T| > 2dC$, there is an attracting and a repelling direction (crossing). The dotted line in the right panel of Figure 10 shows the boundary between the cases of 2 and 4 attracting directions.

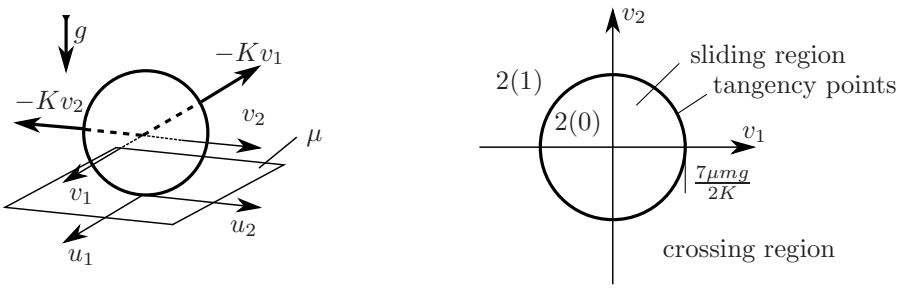

Figure 11. *Ball at the bottom of a pool. Left panel: sketch of the mechanical model with the parameters and state variables. Right panel: sketch of the discontinuity set Σ with the crossing and sliding regions. The meaning of the numbers is the same as in the right panel of Figure 10.*

6.1.3. Sliding dynamics. Let us write (6.6) into the form (5.16), and by choosing $A(\phi) = \cos\phi$, $B(\phi) = \sin\phi$, we get

$$\overline{F} = \begin{pmatrix} -\omega_0^2 d \\ \frac{T}{2md} \\ \frac{T}{2md^2}, \end{pmatrix} \qquad F_A = \begin{pmatrix} -\frac{C}{2m} \\ 0 \\ 0 \end{pmatrix}, \qquad F_B = \begin{pmatrix} 0 \\ -\frac{C}{m} \\ -\frac{C}{md} \end{pmatrix}. \tag{6.11}$$

Then, the solution of (5.20) is

$$a = -\frac{2m\omega_0^2 d}{C}, \qquad b = \frac{T}{2dC}, \tag{6.12}$$

and the sliding vector from (5.18) becomes

$$F_s(x_0) = \begin{pmatrix} 0 \\ 0 \\ \frac{T}{4md^2} \end{pmatrix}. \tag{6.13}$$

This is the same result as we would get from the Newton–Euler equations by assuming that point P is stuck to the plane by static Coulomb friction and the body is rotating around this point.

6.2. Ball at the bottom of a pool. Let us consider a rigid homogeneous ball moving at the bottom of a pool. We assume that Coulomb friction force is acting on the bottom of the ball with a friction coefficient μ, and the effect of the water is modeled by a viscous force with a linear coefficient K (see Figure 11). The mass of the ball is m, the radius of the ball is ρ, and the gravity is denoted by g.

6.2.1. Dynamics. The state of the ball is described by $x = (u_1, u_2, v_1, v_2)$, where u_1 and u_2 are the velocity components of the bottom point and v_1 and v_2 are the velocity components of the center of gravity. The components of the angular velocity of the ball in the horizontal

plane can be expressed by $(u_2 - v_2)/\rho$ and $(v_1 - u_1)/\rho$. Then, for the case when the ball is slipping, Newton's second law for the center of gravity is

$$\begin{aligned} m\dot{v}_1 &= -\mu mg \frac{u_1}{\sqrt{u_1^2 + u_2^2}} - Kv_1, \\ m\dot{v}_2 &= -\mu mg \frac{u_2}{\sqrt{u_1^2 + u_2^2}} - Kv_2, \end{aligned} \tag{6.14}$$

and Euler's equations for the rigid body become

$$\begin{aligned} \frac{2}{5} m\rho^2 \cdot \frac{\dot{u}_2 - \dot{v}_2}{\rho} &= -\mu mg \frac{u_2}{\sqrt{u_1^2 + u_2^2}} \cdot \rho, \\ \frac{2}{5} m\rho^2 \cdot \frac{\dot{v}_1 - \dot{u}_1}{\rho} &= \mu mg \frac{u_1}{\sqrt{u_1^2 + u_2^2}} \cdot \rho, \end{aligned} \tag{6.15}$$

where $2/5m\rho^2$ is the mass moment of inertia of the ball.

By expressing the derivatives of the state variables from (6.14)–(6.15), we get the differential equation

$$\begin{pmatrix} \dot{u}_1 \\ \dot{u}_2 \\ \dot{v}_1 \\ \dot{v}_2 \end{pmatrix} = F(x) = \begin{pmatrix} -\frac{7}{2}\mu g \frac{u_1}{\sqrt{u_1^2+u_2^2}} - \frac{K}{m} v_1 \\ -\frac{7}{2}\mu g \frac{u_2}{\sqrt{u_1^2+u_2^2}} - \frac{K}{m} v_2 \\ -\mu g \frac{u_1}{\sqrt{u_1^2+u_2^2}} - \frac{K}{m} v_1 \\ -\mu g \frac{u_2}{\sqrt{u_1^2+u_2^2}} - \frac{K}{m} v_2 \end{pmatrix}. \tag{6.16}$$

The discontinuity manifold Σ is the hyperplane $u_1 = u_2 = 0$ in the 4D state space. At any point $x_0 = (0, 0, v_{10}, v_{20}) \in \Sigma$, we choose the basis vectors $n_{(1)} = (1, 0, 0, 0)$ and $n_{(2)} = (0, 1, 0, 0)$, which leads to

$$F^*(\phi)(x_0) = \begin{pmatrix} -\frac{7}{2}\mu g \cos\phi - \frac{K}{m} v_{10} \\ -\frac{7}{2}\mu g \sin\phi - \frac{K}{m} v_{20} \\ -\mu g \cos\phi - \frac{K}{m} v_{10} \\ -\mu g \sin\phi - \frac{K}{m} v_{20} \end{pmatrix}. \tag{6.17}$$

The physical meaning of ϕ is the direction of slipping of the bottom point of the ball.

6.2.2. Sliding and crossing regions. For determining the sliding region, let us calculate the functions

$$R(\phi) = -\frac{7}{2}\mu g - \frac{K}{m}\left(v_{10}\cos\phi + v_{20}\sin\phi\right), \qquad V(\phi) = -\frac{K}{m}\left(v_{20}\cos\phi - v_{10}\sin\phi\right). \tag{6.18}$$

The zeroes of $V(\phi)$ are $\phi_1 = \arctan(v_{20}, v_{10})$ and $\phi_2 = \phi_1 + \pi$. The direction ϕ_1 is always an attracting direction while ϕ_2 is attracting only if

$$\sqrt{v_{10}^2 + v_{20}^2} < \frac{7\mu g m}{2K}. \tag{6.19}$$

That is, the sliding region determined by (6.19) is the interior of a circle in the discontinuity set. (See the right panel of Figure 11.) The points of this circle are tangency points and there is crossing outside the circle.

Equation (6.19) gives the same result as could be obtained from applying Newton's second law separately for the case when the ball is rolling at the bottom of the pool and from considering the maximum admissible friction force from the simple Coulomb model.

6.2.3. Sliding dynamics. By choosing $A(\phi) = \cos\phi$ and $B(\phi) = \sin\phi$, the vectors of (5.16) become

$$\overline{F} = \begin{pmatrix} -\frac{K}{m}v_{10} \\ -\frac{K}{m}v_{20} \\ -\frac{K}{m}v_{10} \\ -\frac{K}{m}v_{20} \end{pmatrix}, \qquad F_A = \begin{pmatrix} -\frac{7}{2}\mu g \\ 0 \\ -\mu g \\ 0 \end{pmatrix}, \qquad F_B = \begin{pmatrix} 0 \\ -\frac{7}{2}\mu g \\ 0 \\ -\mu g \end{pmatrix}. \tag{6.20}$$

The solution of (5.20) leads to

$$a = -\frac{2Kv_{10}m}{7\mu g}, \qquad b = -\frac{2Kv_{20}m}{7\mu g} \tag{6.21}$$

and to the sliding vector

$$F_s = \begin{pmatrix} 0 \\ 0 \\ -\frac{5}{7}\frac{K}{m}v_{10} \\ -\frac{5}{7}\frac{K}{m}v_{20} \end{pmatrix}. \tag{6.22}$$

This vector field describes the ball during rolling on the ground, and the equation is consistent with the one obtained from Newton's second law in the rolling case.

6.2.4. Planar case—Comparison to simple Filippov systems. Let us demonstrate that the results are consistent also to those from simple Filippov systems. By applying the constraints $u_2 \equiv v_2 \equiv 0$, (6.16) becomes

$$F(x) = \begin{pmatrix} -\frac{7}{2}\mu g \operatorname{sgn} u_1 - \frac{K}{m}v_1 \\ 0 \\ -\mu g \operatorname{sgn} u_1 - \frac{K}{m}v_1 \\ 0 \end{pmatrix}, \tag{6.23}$$

which is a Filippov system describing the problem in two dimensions. By applying the methods described in section 2, we obtain $F_s = (0, 0, -5Kv_{10}/(7m), 0)$ and $|v_{10}| < (7\mu g m)/(2K)$, which coincide with (6.22) and (6.19).

6.3. Regularization of the Coulomb friction model. By considering a small positive parameter ϵ, the planar (2D) Coulomb model (6.2) can be approximated by

$$C_1 = \begin{cases} -\mu N u_1/\epsilon & \text{if } |u_1| < \epsilon, \\ -\mu N u_1/|u_1| & \text{if } |u_1| \geq \epsilon. \end{cases} \tag{6.24}$$

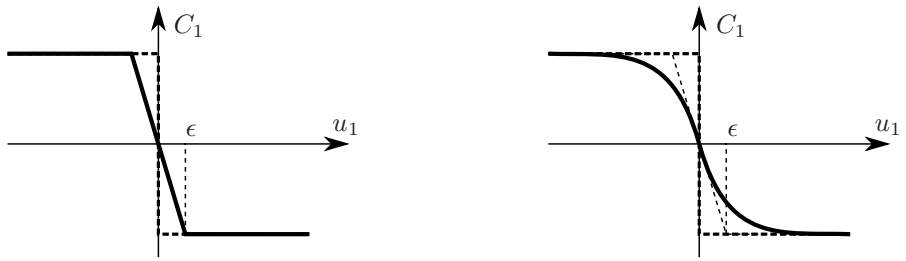

Figure 12. *Different regularizations of the Coulomb friction model* (6.1). *Left panel: piecewise linear regularization from* (6.24). *Right panel: smooth regularization by the* tanh *function from* (6.25). *These models for the planar (2D) friction can be extended to the spatial (3D) case in the form* (6.26) *and* (6.27).

This formulation provides a piecewise linear model, where the discontinuity at $u_1 = 0$ is eliminated (see Figure 12). Note that the model is still not smooth at $|u_1| = \epsilon$. A different way to regularize (6.2) is to use a smooth approximating function, e.g., in the form

$$C_1 = -\mu N \frac{u_1}{|u_1|} \cdot \tanh\left(\frac{|u_1|}{\epsilon}\right) = -\mu N \tanh\left(\frac{u_1}{\epsilon}\right). \tag{6.25}$$

The formula (6.24) fits into the framework of the regularization according to Sotomayor and Teixeira [21]. Thus, the *mathematical* reason behind this regularization is to analyze the dynamics in the discontinuity set by blowing up the single surface into a boundary layer. However, there is a *physical* justification behind these regularized models, as well. If the normal force N between rolling bodies is large enough compared to the local stiffness of the bodies, then the local deformation at the contact point cannot be neglected. From the point of view of the rigid body motion, this effect of *creep* appears as a slight slipping between the rolling surfaces. Then, the value $1/\epsilon$ gets the physical meaning of the *linear creep coefficient*, which can be calculated from the mechanical analysis of the elastic deformations (see [16, p. 242]).

The regularized models (6.26) and (6.27) can be extended to the 3D Coulomb friction, and we get

$$C_1 = \begin{cases} -\mu N u_1/\epsilon & \text{if } \sqrt{u_1^2+u_2^2} < \epsilon, \\ -\mu N \frac{u_1}{\sqrt{u_1^2+u_2^2}} & \text{if } \sqrt{u_1^2+u_2^2} \geq \epsilon, \end{cases} \tag{6.26}$$

or

$$C_1 = -\mu N \frac{u_1}{\sqrt{u_1^2+u_2^2}} \tanh\left(\frac{1}{\epsilon}\sqrt{u_1^2+u_2^2}\right), \tag{6.27}$$

where the component C_2 can be written into a similar form. By taking $\epsilon \to 0$, both models (6.26) and (6.27) tend to (6.1). In the case of (6.26), a *boundary tube* with a diameter of 2ϵ appears around the codimension-2 discontinuity manifold of the original system. The model (6.27) provides a smooth friction model.

The form of the formulae (6.26)–(6.27) can be used for the regularization not just in systems originated in mechanical applications but in other Filippov systems as in the examples

mentioned before. By approximating the nonsmooth terms as in (6.27) in Examples 4.4 and 4.7, the origin of the projected phase space becomes a stable node and a stable focus, respectively.

In the regularized system obtained from Example 4.5, there is a stable node and a saddle close to each other. This result harmonizes with the phase portrait of the original system in polar coordinates. (See the left-bottom diagram in Figure 4.) That is, there are trajectories in the regularized system which tend to the stable node and which are not leaving along the repelling direction. This example demonstrates that the analysis of the regularized system can be important at points with several limit directions. Definitions 5.1 and 5.4 of crossing and sliding are based purely on the existence of the attracting and repelling limit trajectories. An appropriate regularization can show more details about the connection between the trajectories at the discontinuity manifold.

By reversing the direction of time in Example 4.5, we get a system where there are more than one repelling limit directions. In that case, the uniqueness of the solution in forward time is violated. By the regularization (6.27), an unstable node and a saddle appear in that system. Depending on the initial condition, the trajectories follow different repelling directions, and thus, the nonuniqueness is resolved by the regularization. It is an open question whether this situation of more than one repelling direction can be obtained from a mechanical system with spatial Coulomb friction. So far, the authors have not found such an example.

This subsection simply gave some ideas about the regularization of extended Filippov systems. It can be the topic of further research to investigate whether the recent results of the regularization of simple Filippov systems (see, e.g., [17]) can be modified and applied to extended Filippov systems.

7. Conclusion.

Motivated by the spatial Coulomb friction, we defined the concept of *extended Filippov systems*, where there are isolated codimension-2 discontinuities in the phase space. Unlike in simple Filippov systems, there are not only two, but continuously many directions normal to the discontinuity manifold at any point. By introducing the notion of limit trajectories, the points of the discontinuity set can be classified into sliding and crossing regions, tangency points, and center points. From the *limit vector field* at a chosen point of the discontinuity set, one can decide the region where the chosen point is located.

In the sliding region, the sliding dynamics is considered as a weighted integral average of the limit vector field, which is analogous to the convex combination at simple Filippov systems. We proved that in the sliding region, such a sliding vector always exists, but there are continuously many choices in general. The subset of systems with unique sliding vector is important, because mechanical problems tend to result this type of systems.

The developed tools of extended Filippov systems are demonstrated on two mechanical problems with spatial Coulomb friction. The resulting conditions of sliding (mechanical sticking/rolling) and crossing (mechanical slipping) are consistent to the results from computing the friction forces directly. That is, extended Filippov systems can have the same role when modeling spatial Coulomb friction as that of the simple Filippov systems at systems with planar Coulomb friction.

These results of the paper present the foundations of the theory and many questions are still open. It would be interesting to see whether the nonuniqueness of the sliding vector

can be resolved by similar methods to that of the intersecting discontinuity manifolds of simple Filippov systems (see [15]). It would be important to extend also the categorization of boundary equilibrium bifurcations (see, e.g., [14]) to the codimension-2 discontinuity. The numerical methods of piecewise smooth systems (see, e.g., [20]) could also be generalized for extended Filippov systems. The recent results about the regularization methods (see, e.g., [17]) could possibly be used for extended Filippov systems, as well. Finally, it could be interesting to see if the spatial Coulomb friction is the only practical source of this type of discontinuity or there are other applications which result to extended Filippov systems.

Acknowledgments. The authors wish to thank Professor S. John Hogan from the University of Bristol for the useful discussions about the topic. We also thank Elena Bossolini from the Technical University of Denmark for the suggestions about the literature of blowup methods.

REFERENCES

[1] M. Antali and G. Stepan, *Discontinuity-induced bifurcations of a dual-point contact ball*, Nonlinear Dynam., 83 (2016), pp. 685–702.
[2] M. Antali and G. Stepan, *Loss of stability in a nonsmooth model of dual-point rolling*, in The Dynamics of Vehicles on Roads and Tracks, CRC Press/Balkema, the Netherlands, 2016, pp. 937–946.
[3] M. Antali and G. Stepan, *Sliding dynamics on codimension-2 discontinuity surfaces*, in Extended Abstracts Spring 2016, Trends Math. 8, Birkhäuser, Basel, pp. 7–12.
[4] J. A. Batlle, *The sliding velocity flow of rough collisions in multibody systems*, J. Appl. Mech., 63 (1996), pp. 804–809.
[5] A. P. da Costa and A. Seeger, *Cone-constrained eigenvalue problems: Theory and algorithms*, Comput. Optim. Appl., 45 (2010), pp. 25–57.
[6] M. di Bernardo, C. J. Budd, A. R. Champneys, and P. Kowalczyk, *Piecewise-Smooth Dynamical Systems*, Springer, New York, 2008.
[7] L. Dieci and F. Difonzo, *The moments sliding vector field on the intersection of two manifolds*, J. Dynam. Differential Equations, 29 (2017), pp. 169–201.
[8] L. Dieci, C. Elia, and L. Lopez, *A Filippov sliding vector field on an attracting co-dimension 2 discontinuity surface, and a limited loss-of-attractivity analysis*, J. Differential Equations, 254 (2013), pp. 1800–1832.
[9] L. Dieci and L. Lopez, *Sliding motion on discontinuity surfaces of high co-dimension. a construction for selecting a Filippov vector field*, Numer. Math., 117 (2011), pp. 779–811.
[10] F. Dumortier, *Singularities of vector fields of the plane*, J. Differential Equations, 23 (1977), pp. 53–106.
[11] A. F. Filippov, *Differential Equations with Discontinuous Righthand Sides*, Kluwer Acacemic Publishers, Dordrecht, the Netherlands, 1988.
[12] C. Glocker, *Formulation of spatial contact situations in rigid multibody systems*, Comput. Methods Appl. Mech. Engrg., 177 (1999), pp. 199–214.
[13] C. Glocker, *Set-Valued Force Laws*, Springer, New York, 2001.
[14] S. J. Hogan, M. E. Homer, M. R. Jeffrey, and R. Szalai, *Piecewise smooth dynamical systems theory: The case of the missing boundary equilibrium bifurcations*, J. Nonlinear Sci., 26 (2016), pp. 1161–1173.
[15] M. R. Jeffrey, *Dynamics at a switching intersection: Hierarchy, isonomy, and multiple sliding*, SIAM J. Appl. Dyn. Syst., 13 (2015), pp. 1082–1105.
[16] K. L. Johnson, *Contact Mechanics*, Cambridge University Press, Cambridge, 1985.
[17] K. U. Kristiansen and S. J. Hogan, *On the use of blowup to study regularizations of singularities of piecewise smooth dynamical systems in r3*, SIAM J. Appl. Dyn. Syst., 14 (2015), pp. 382–422.
[18] C. Kuehn, *Multiple Time Scale Dynamics*, Springer, New York, 2015.

[19] R. I. Leine and C. Glocker, *A set-valued force law for spatial Coulomb–Contensou friction*, Eur. J. Mech. A Solids, 22 (2003), pp. 193–216.
[20] P. T. Piiroinen and Y. A. Kuznetzov, *An event-driven method to simulate Filippov systems with accurate computing of sliding motions*, ACM Trans. Math. Software, 34 (2008), pp. 1–24.
[21] J. Sotomayor and M. A. Teixeira, *Regularization of discontinuous vector fields*, in Proceedings of the International Conference on Differential Equations, Lisboa, Equadiff 95, 1996, pp. 207–223.
[22] G. Stepan, *Chaotic motion of wheels*, Vehicle Syst. Dyn., 20 (1991), pp. 341–351.
[23] V. I. Utkin, *Sliding Modes in Control and Optimization*, Springer, New York, 1992.